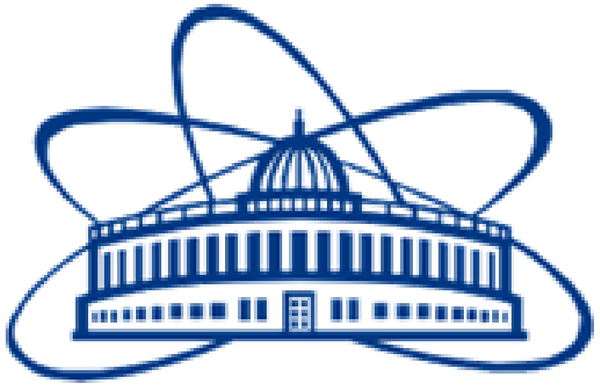

JOINT INSTITUTE FOR NUCLEAR RESEARCH
VEKSLER AND BALDIN LABORATORY OF HIGH ENERGY PHYSICS

FINAL REPORT ON THE INTEREST PROGRAMME

DESCRIPTION OF MPD, MINIBEBE, AND READOUT ELECTRONICS

SUPERVISOR:
DR IVONNE ALICIA MALDONADO CERVANTES

STUDENT:
JESUS ARMANDO CERNA NUÑEZ
THE UNIVERSITY MICHOACANA DE SAN NICOLÁS DE HIDALGO

PARTICIPATION PERIOD:
FEBRUARY 20– APRIL 22, WAVE 10, 2024

Description MPD(Multi Purpose Detector)

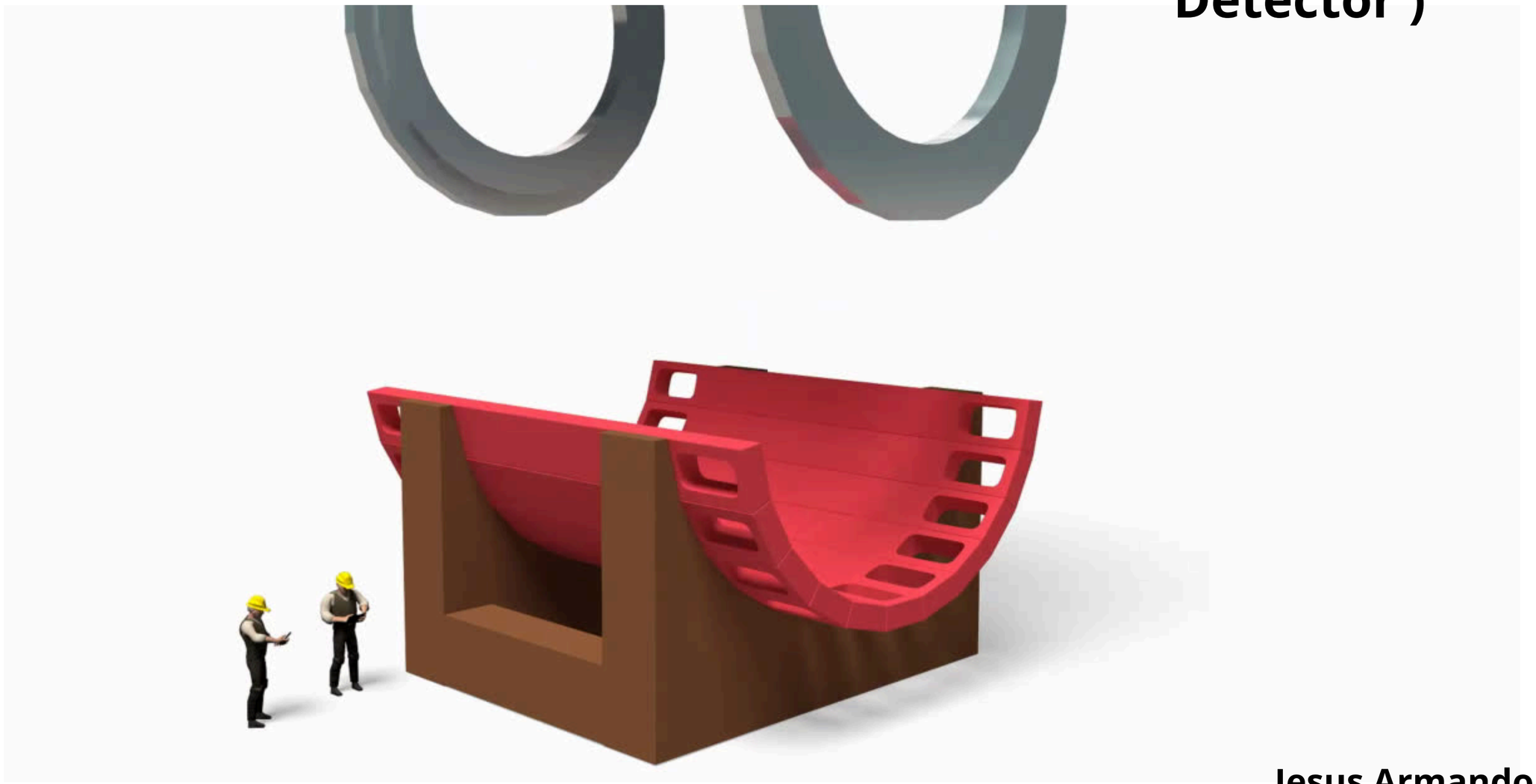

Jesus Armando Cerna Nuñez

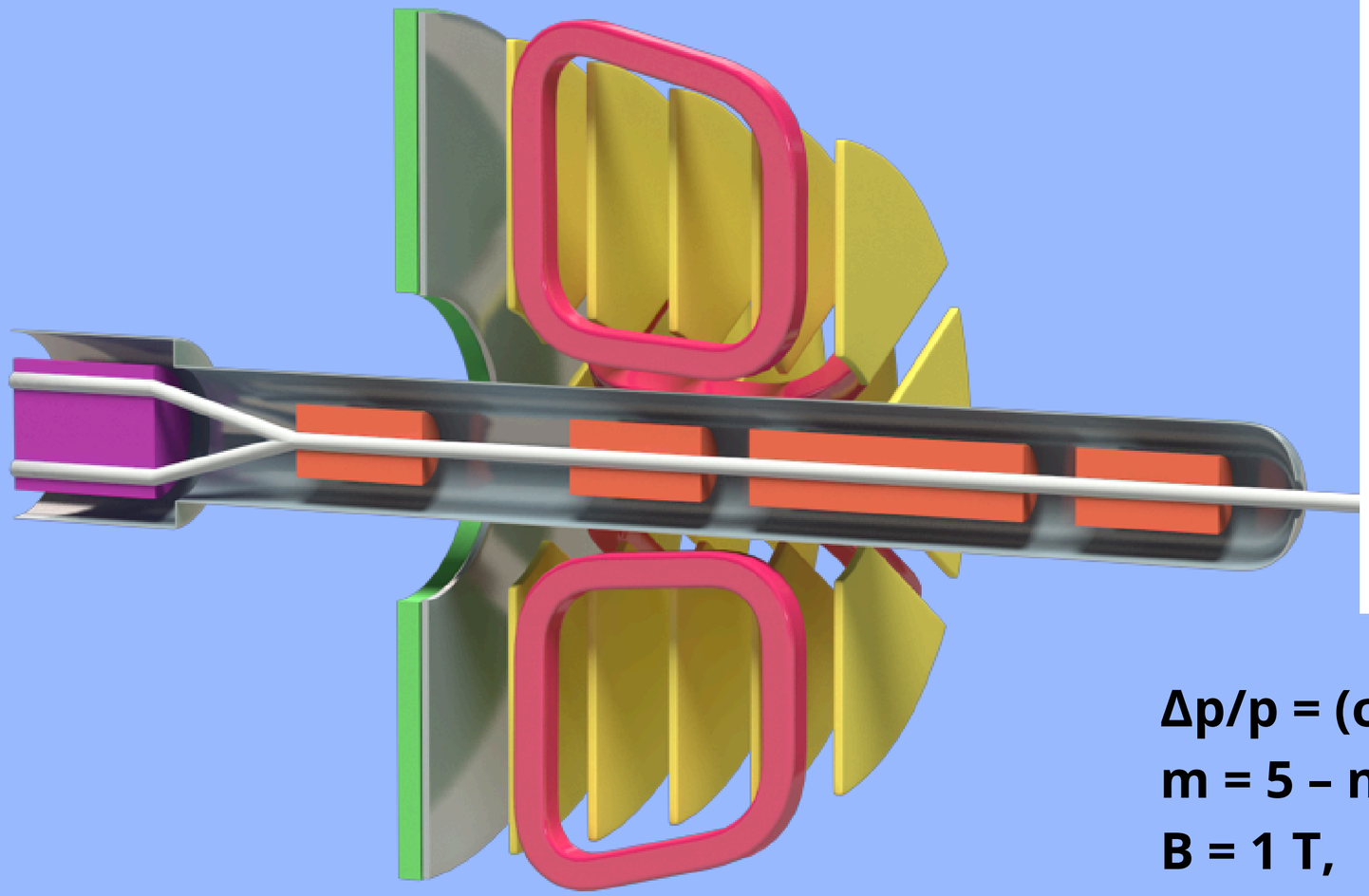

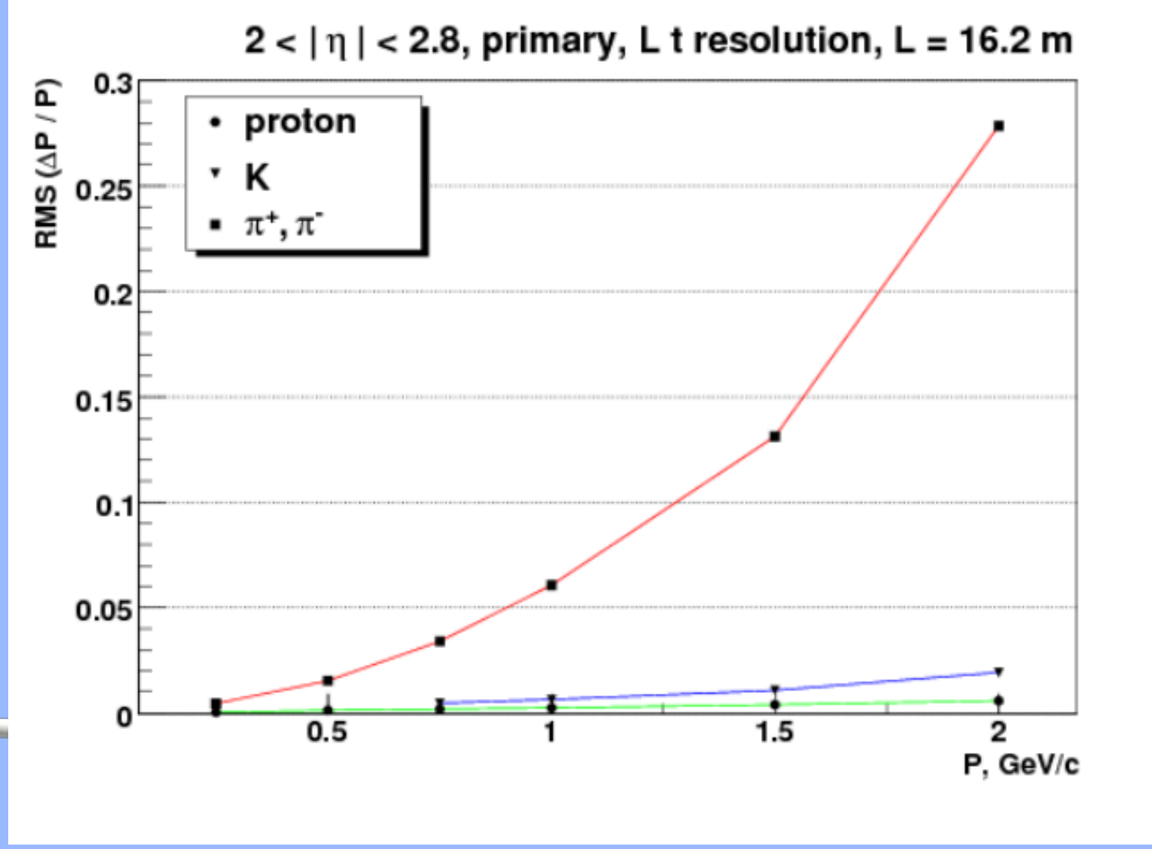

Δp/p = (σ/Lp2)(pp/0.2998B) p [720/(m + 6)].

m = 5 – number of measurements along the track

B = 1 T,

σ = 200 μm,

L = 1 m,

p = 1 GeV/c ΔP/P ~ 1.7%

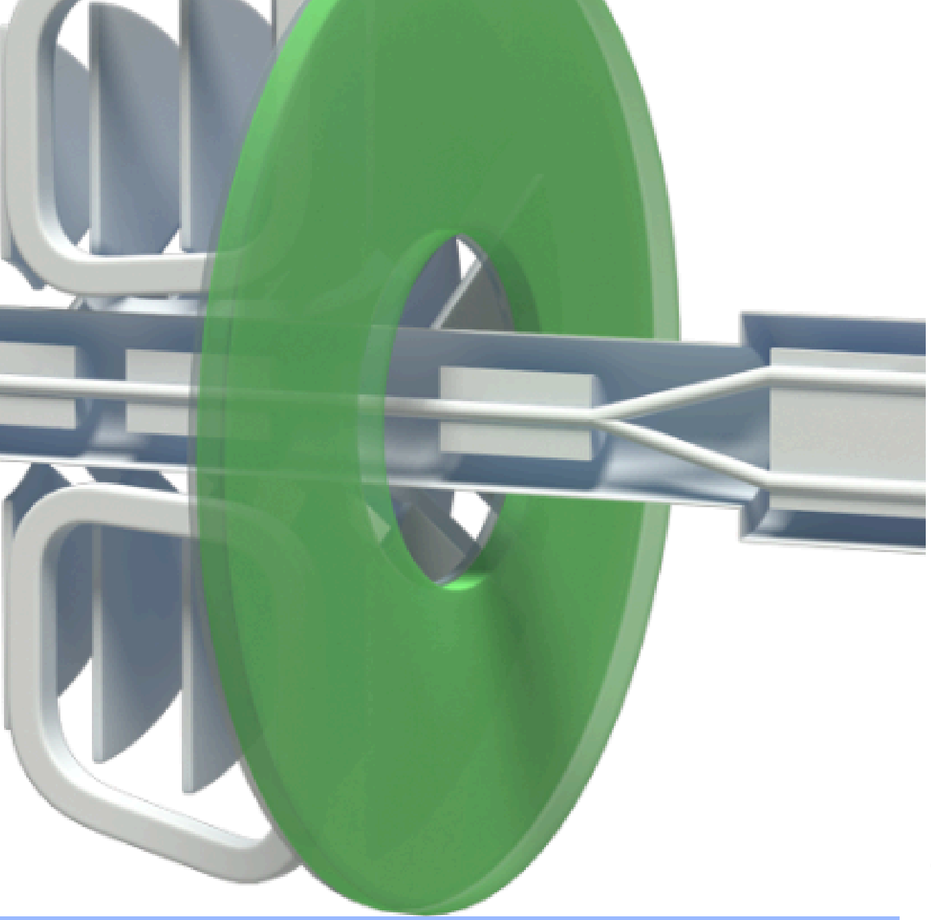

Fig. 1: Mass separation with TOF (100 ps resolution).

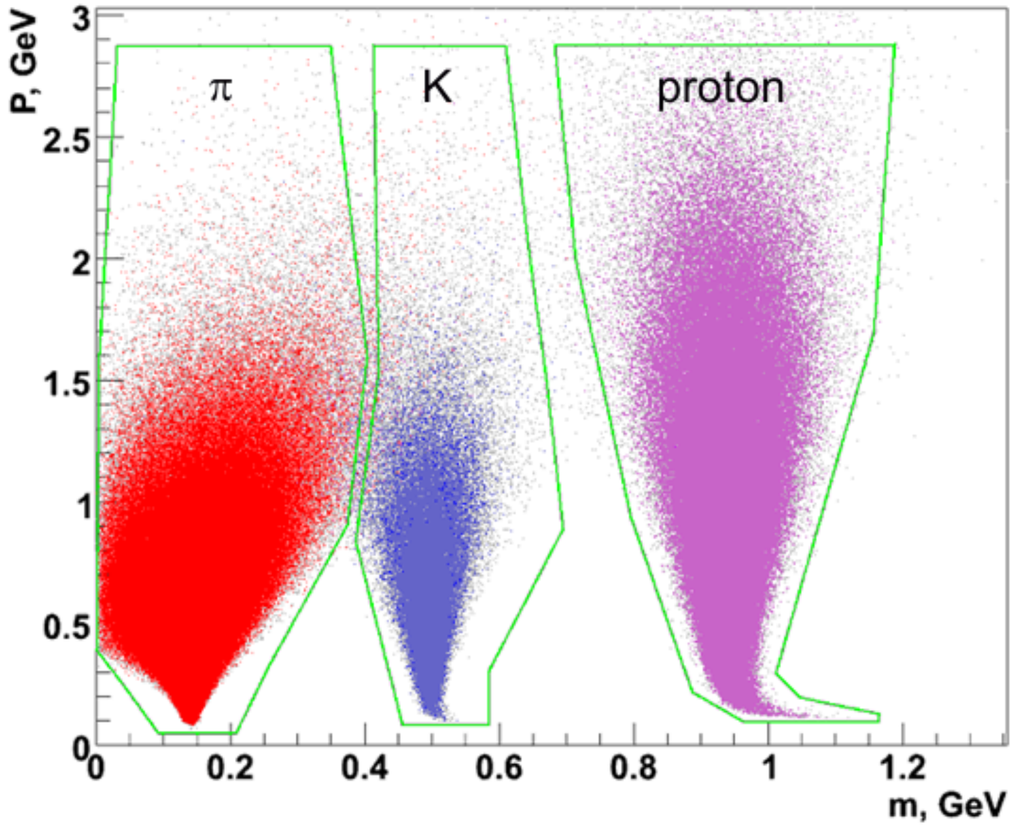

TIME OF FLY SYSTEM (TOF)

The basic requirements to the TOF system are:

– large phase space coverage $|\eta| < 2$;

– high granularity to keep the overall system occupancy below 10–15% and minimize efficiency degradation due to double hits;

– good position resolution to provide effective matching of TOF hits with TPC tracks;

– high combined geometrical and detection efficiency (better than 80%);

– identification of pions and kaons with $0.1 < pt < 2$ GeV/c;

– identification of (anti)protons with $0.3 < pt < 3$ GeV/c;

– TOF detector elements must function in a 0.5 T magnetic field.

Multi-Purpose Detector (MPD)

central detector

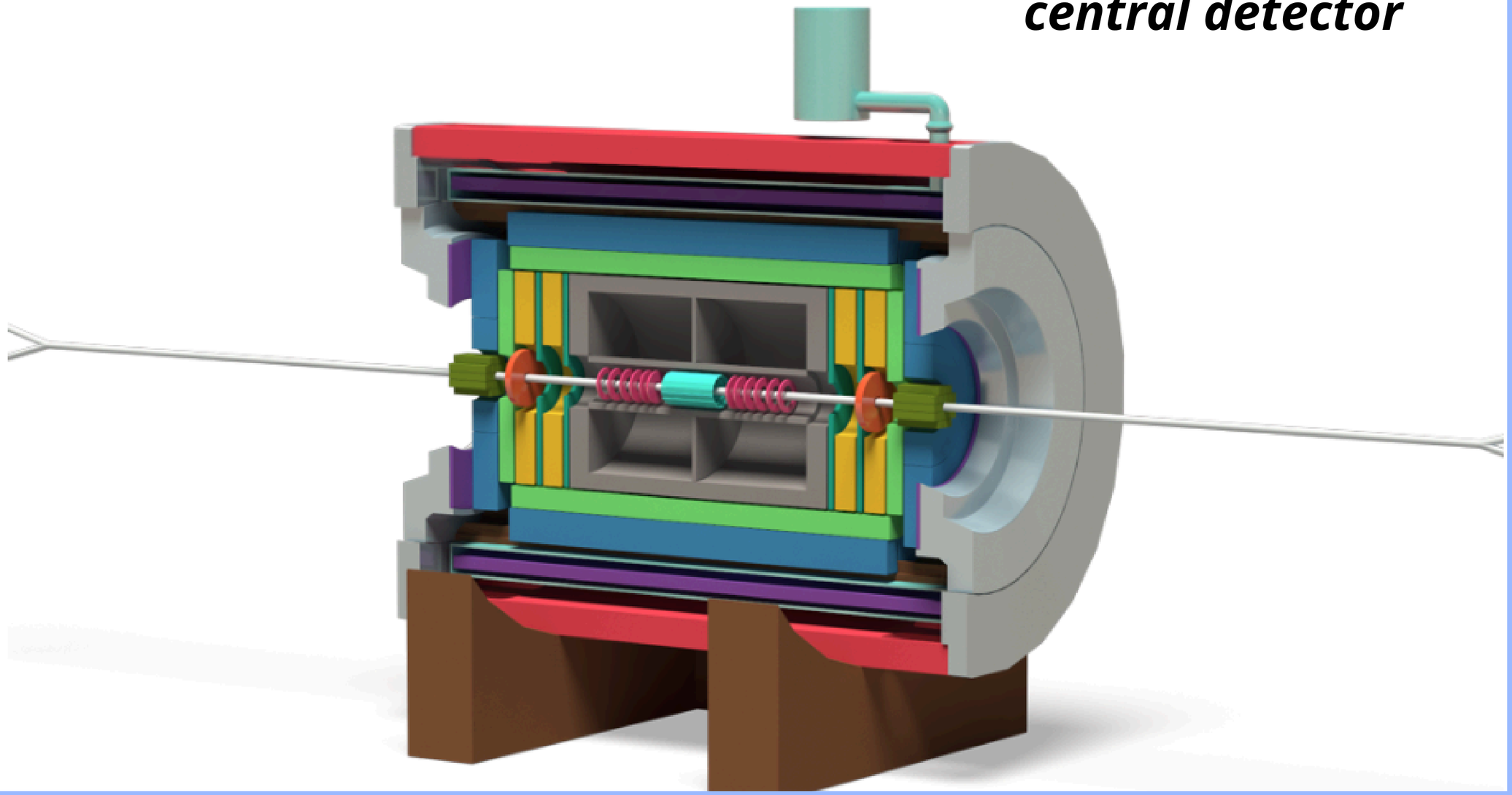

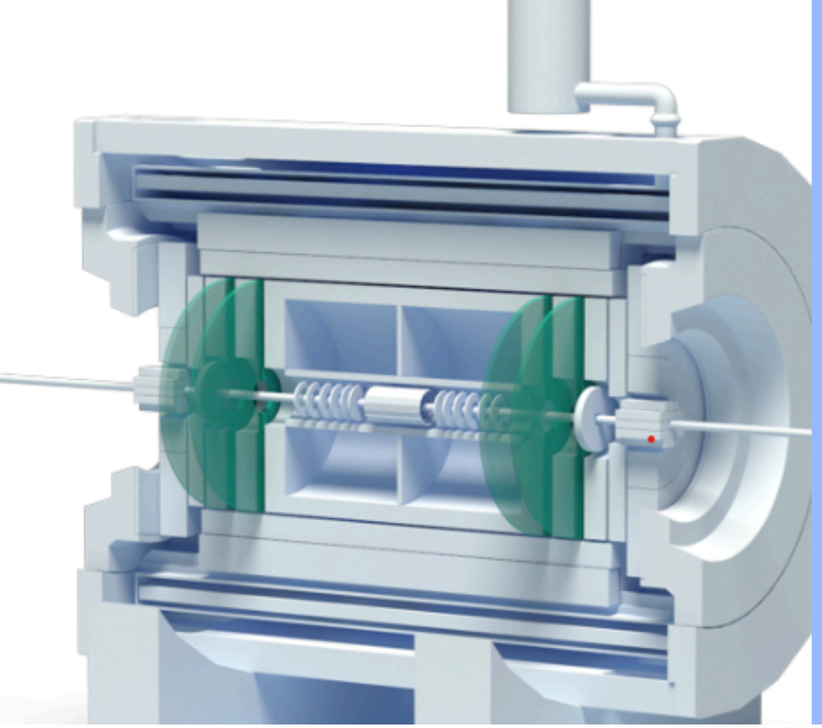

The basic elements for the CPC construction are a module panels. The procedure of module construction as follow:

— the high modulus skins of Carbon Fiber Composite (CFC) glued on both sides of 10 mm thick core of ROHACELL 31 HF [271] foam;
— to ensure the sealing of the gas box and its electrical shielding and grounding, a thin laminate of Kapton and Aluminium will be added to both sides of the panel;
— the FR-4 printed boards with cathode pad structure will be glued after that to both sides of the panel;
— at each end of the module panel, an insert will be glued, sandwiched between the two CFC.

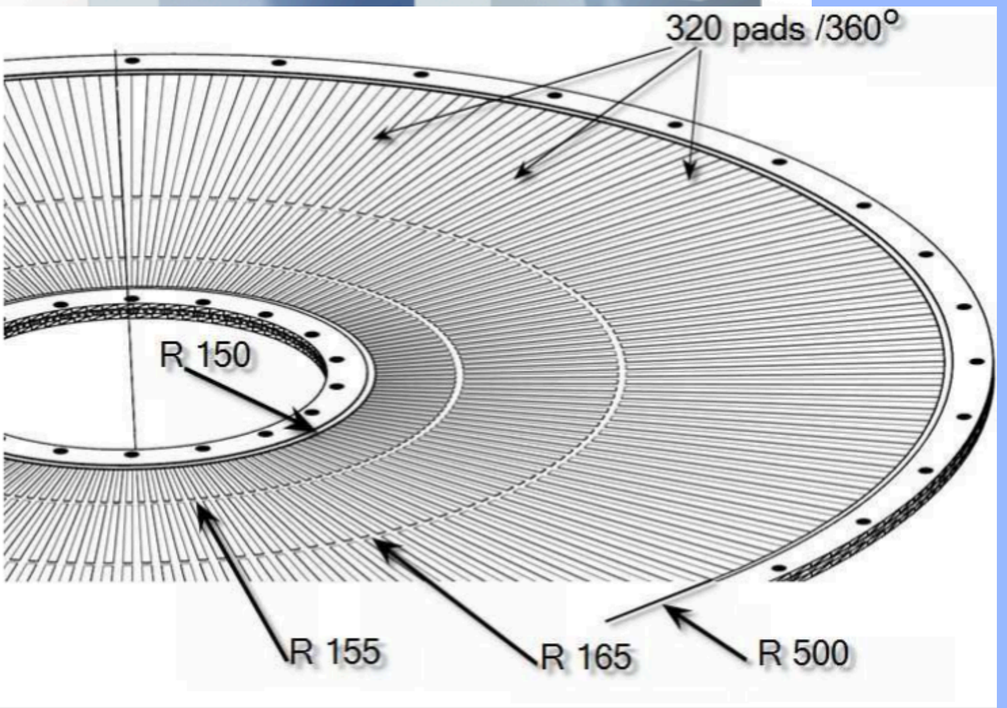

Fig. 1: Layout of an CPC cathode pad structure in ϕ.

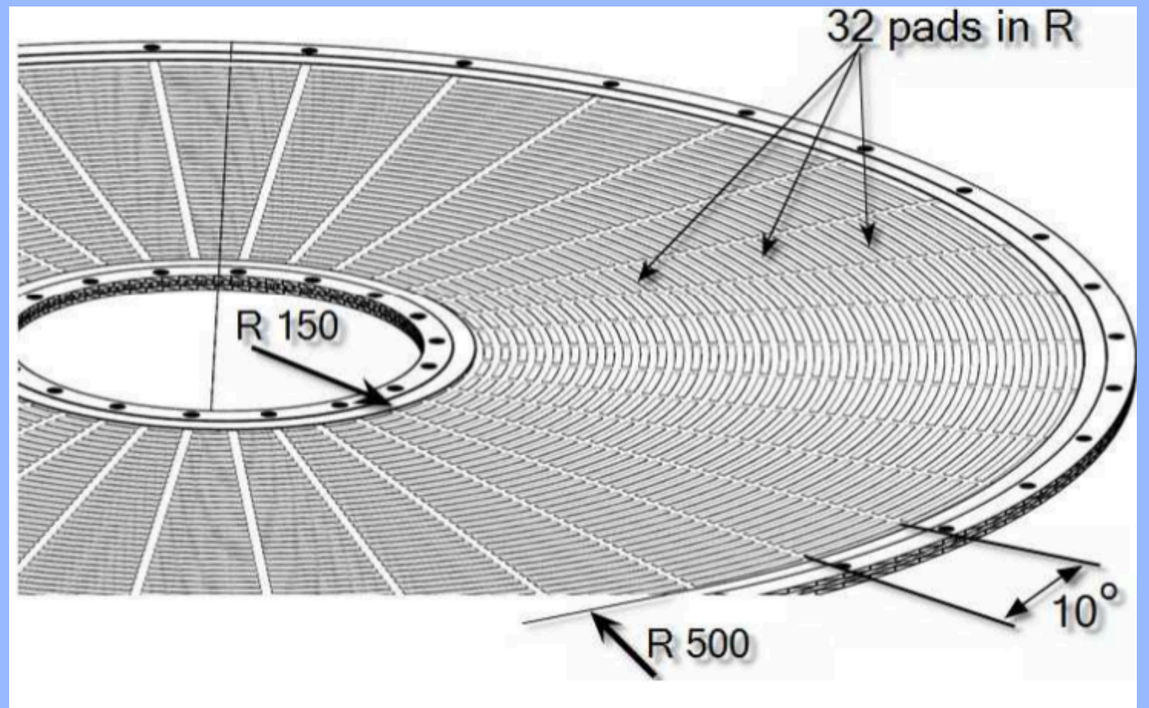

Fig. 2: Layout of an CPC cathode pad structure in R.

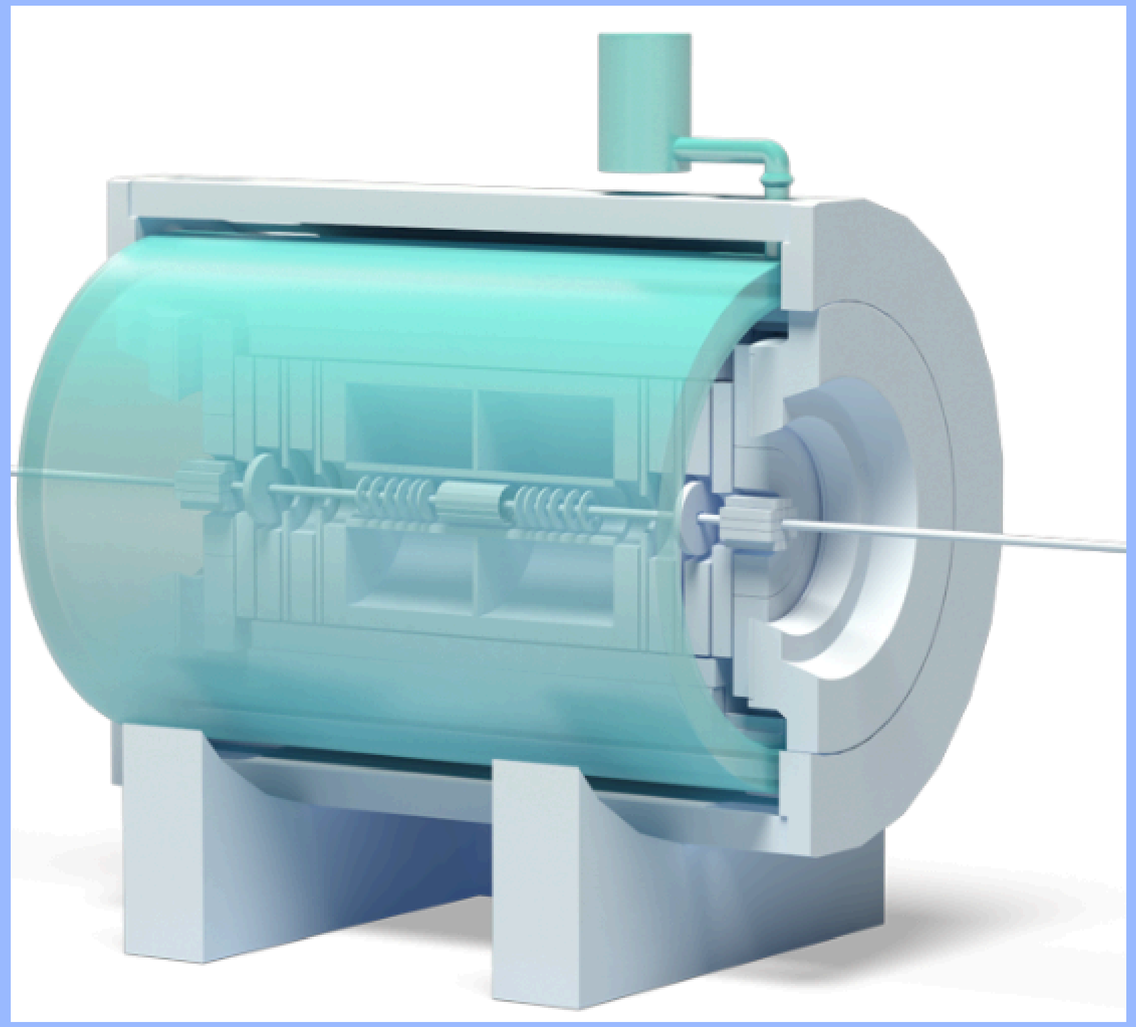

Cryostat

To obtain the assured thermal stabilization of the conductor, the cold mass is to be installed in the space between inner and outer cryostat vacuum shells and supported by high thermal resistance ties and struts. The coil is indirectly cooled by two-phase liquid helium flowing through an aluminum cooling tube, which is welded to the outside surface of the support cylinder. The cold volume is surrounded by the thermal shield supported from the side of the vacuum chamber, which is cooled by helium gas at 40-80 K.

The cryostat is equipped with radiation shield inserted between the coil and the cryostat outer can. The shield surface is covered by high purity aluminum foil to reduce radiation heat loads. About 30 layers of superinsulation separate the vacuum vessel walls from the shields. The data of the thermal load at the thermal shield multiplied by the safety factor 2 . The overall heat load at the level 77 K is expected not to exceed 734 W in the operational mode.

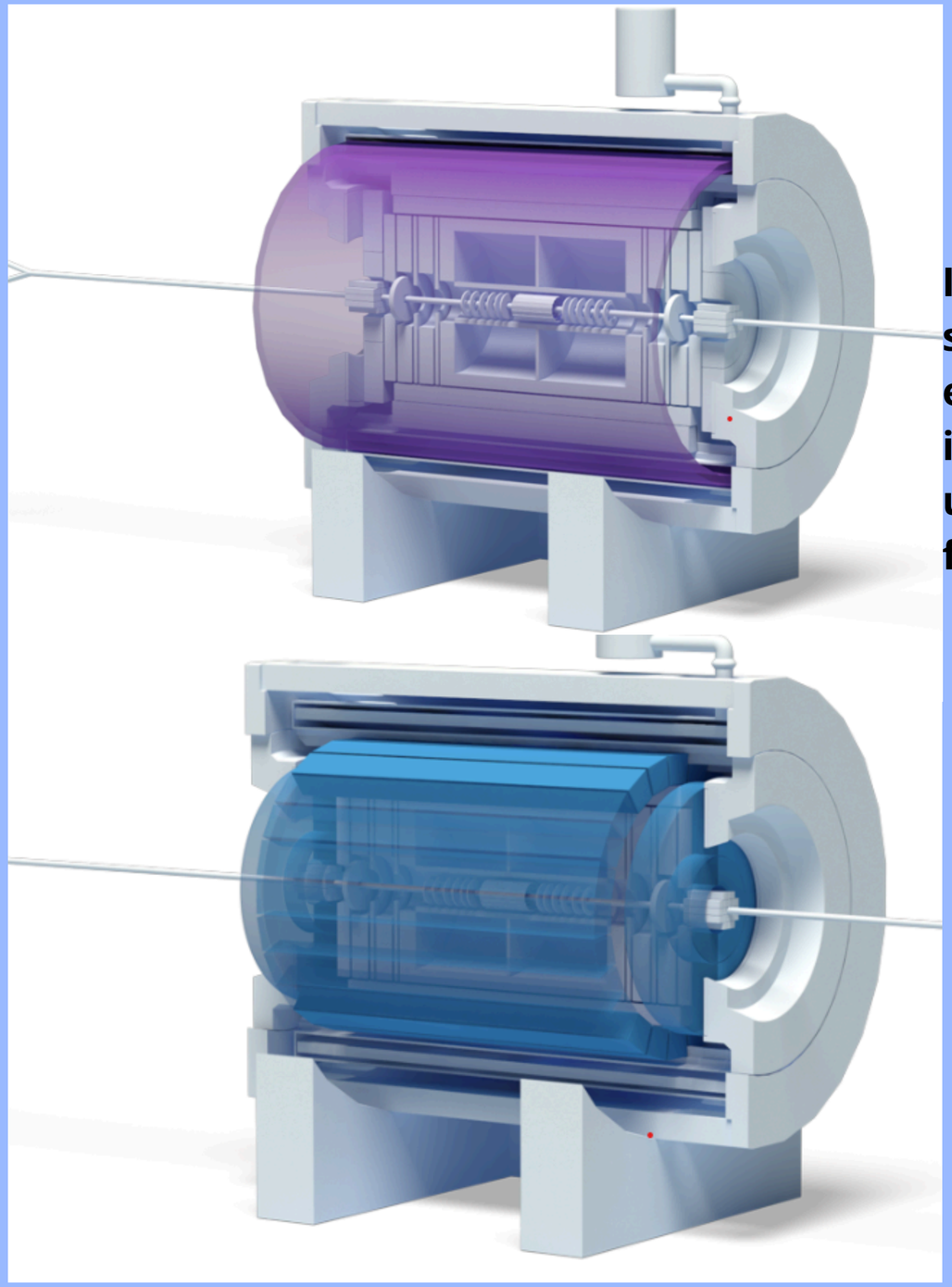

ECal The whole barrel part of MPD electromagnetic calorimeter will be constructed from 48 sectors (Fig.1). The heat-producing electronics will be thus separated from the modules and mounted on the upper parts of sectors.

In the case of the MPD, the ECal will be constructed with multiple sectors, and it is expected to provide precise measurements of the energy of electromagnetic particles interacting with it. This information is essential for understanding the physical processes under study and for identifying new particles and phenomena in the field of particle physics.

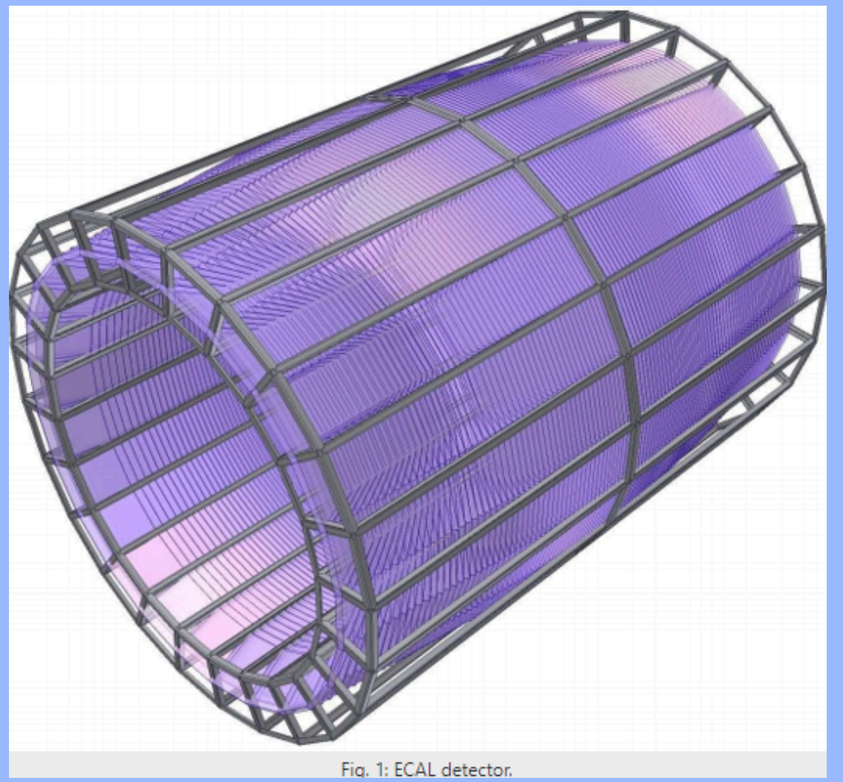

Fig. 1: ECAL detector.

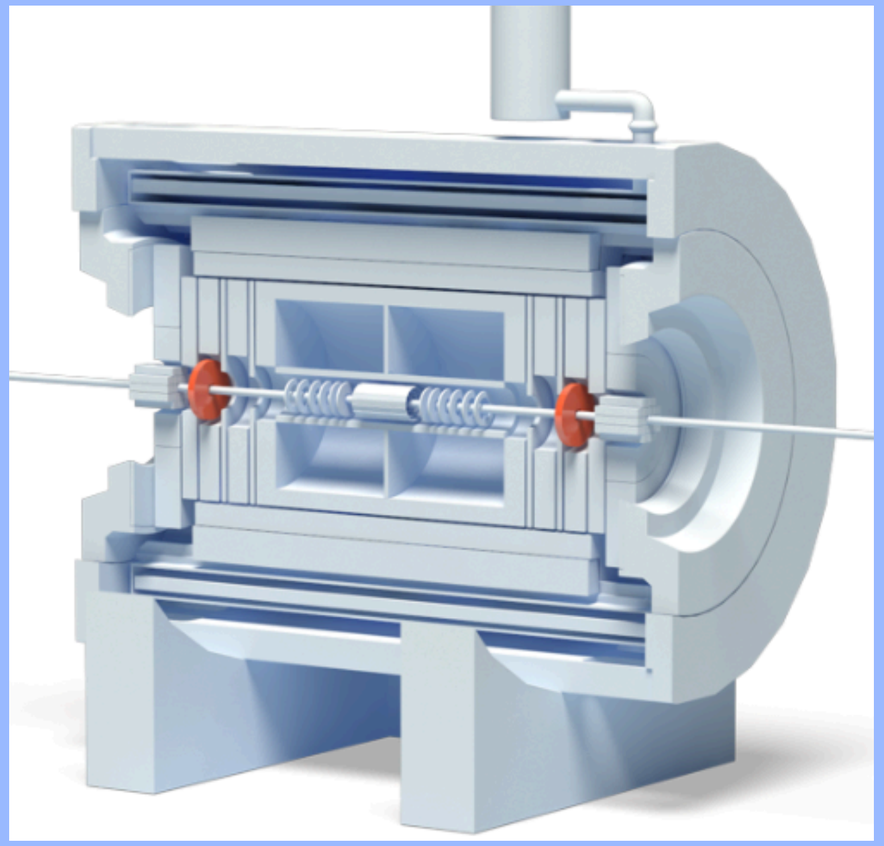

FD

Main aims of the FFD are fast determination of a nucleus-nucleus interaction in the center of the MPD setup. Besides, there are some additional important tasks where FFD is a useful instrument. It can much help in adjustment of beam-beam collisions in the center of the MPD and operative control of the collision rate and interaction point position during a run.

In comparison with experiments at ultra-relativistic energies at RHIC and LHC, there are two essential difficulties at the NICA energies. First, the charged particles produced in collisions mainly are not relativistic, and there is a large spread of spectator velocities which differ from the velocity of light (the beam velocities are in an interval $0.78 \leq \beta \leq 0.98$). Second, the particle multiplicity is much lower than one in the other collider experiments. As a result, for efficient trigger we need to cover a large acceptance and try to detect all particles with β 1 to achieve needed timing. It leads to conclusion that the trigger and timing detectors used in other experiments at higher energies are not an optimal solution in our case and do not allow to reach the requirements mentioned above. So, one has to develop another conception of trigger and timing detectors for the MPD experiment.

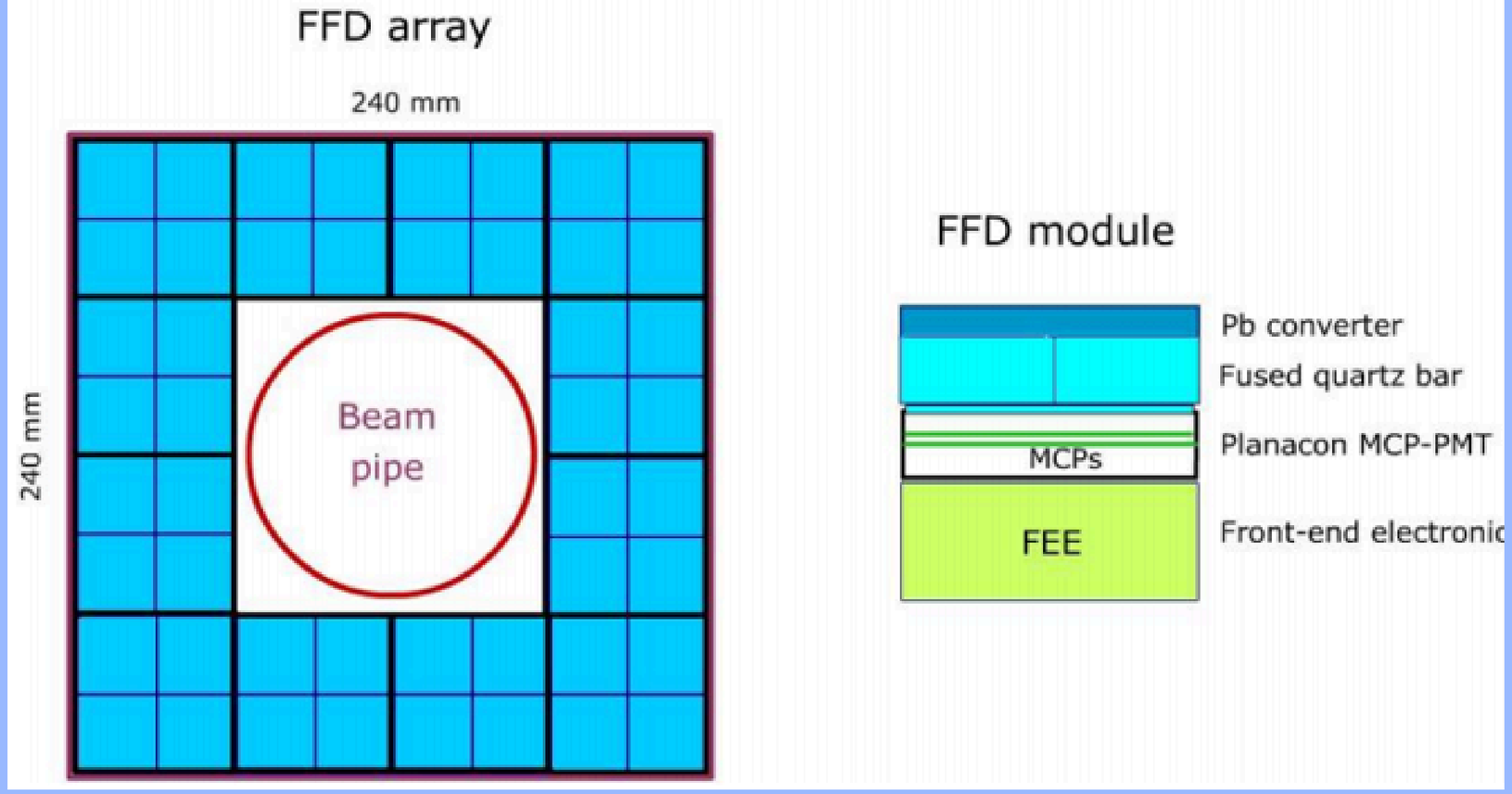

There is a well-known fact that central and semi-central collisions of two heavy nuclei at relativistic energies are characterized by multiple pion production. The neutral pions immediately decay with generation of many high energy photons passing the MPD subdetectors. The main idea of the FDD is to register a part of these photons at small angles to beam axis as the most suitable secondaries with highest and constant velocity. The proposed FFD design is a granulated Cherenkov detector which has a high efficiency for the high energy photons and for ultra-relativistic charged particles as well. The FFD consists of two sub-detectors, FFD-L and FFD-R, which are symmetrically placed to the MPD center along the beam line. Each sub-detector array has a hole for the beam pipe and locates at a distance of 75 cm from the center. Its acceptance in pseudo-rapidity is $2.5 \leq |\eta| \leq 3.2$.

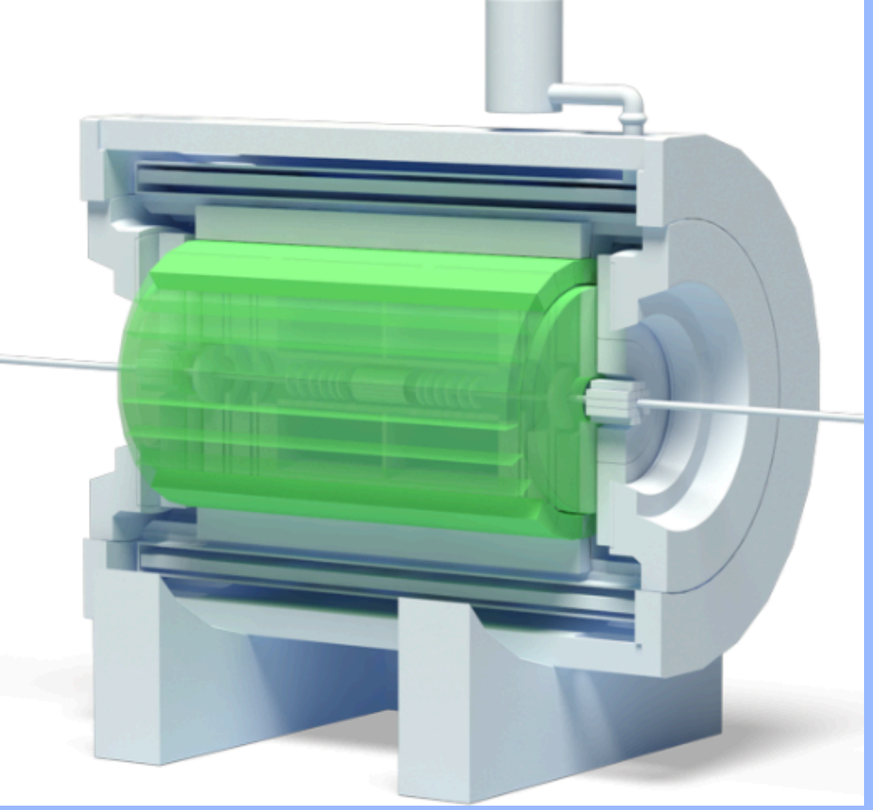

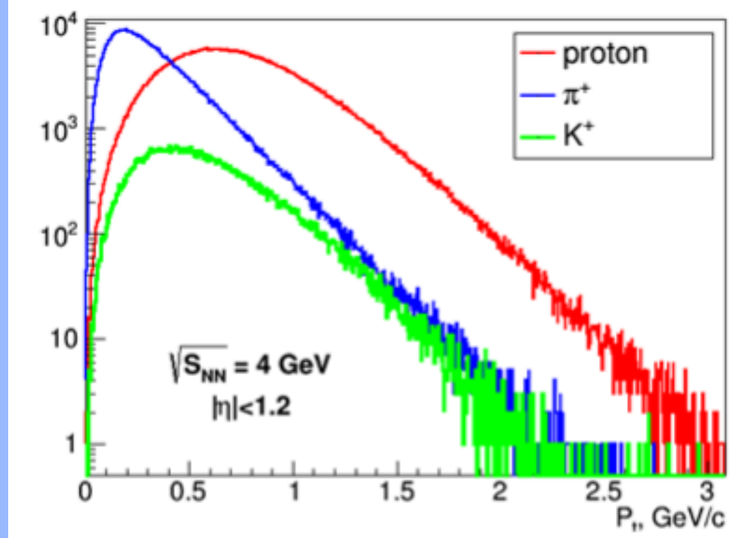

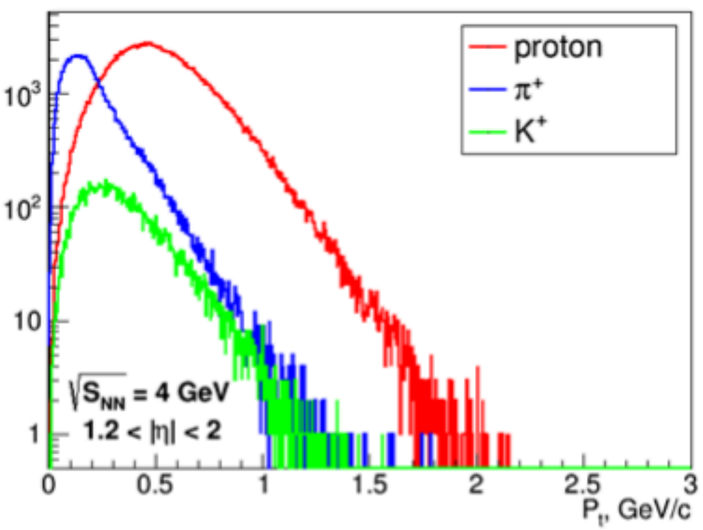

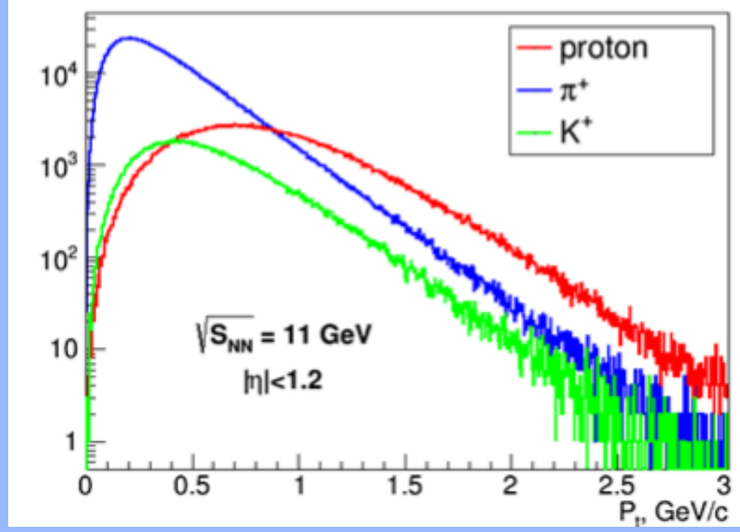

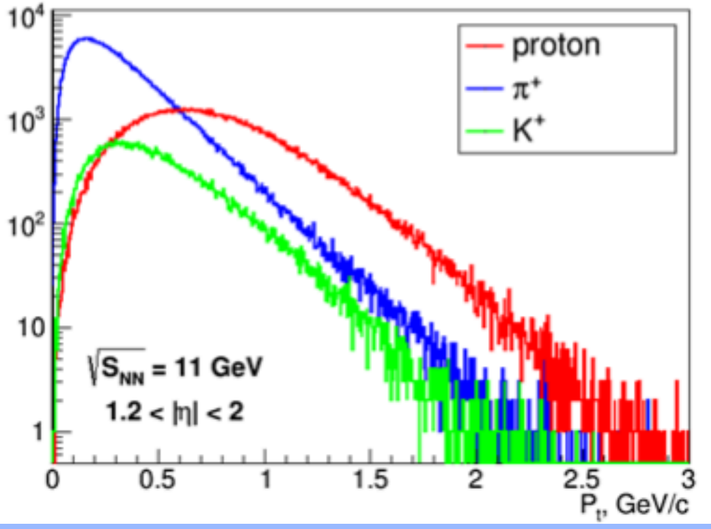

At the relatively high momenta of particles the errors in time of flight measurement and track length definition have higher weight than the error of momentum determination. The momentum spectra of secondary particles at the NICA colliding energies produced in the regions of pseudorapidity $|\eta| < 1.2$ and $1.2 < |\eta| < 2$ for minimum (4 GeV) and maximum (11 GeV) colliding energies are presented on the Fig. The average momentum of pions for energy 4 GeV is about 300 MeV/c and for 11 GeV is about 400 MeV/c.

The smallest track length for time of flight measurement at MPD is 1.5 m. We expect to have overall time resolution better than 100 ps. It allows us reliable separation of pions, kaons and protons in the entire interval of momenta for produced particles for NICA energies

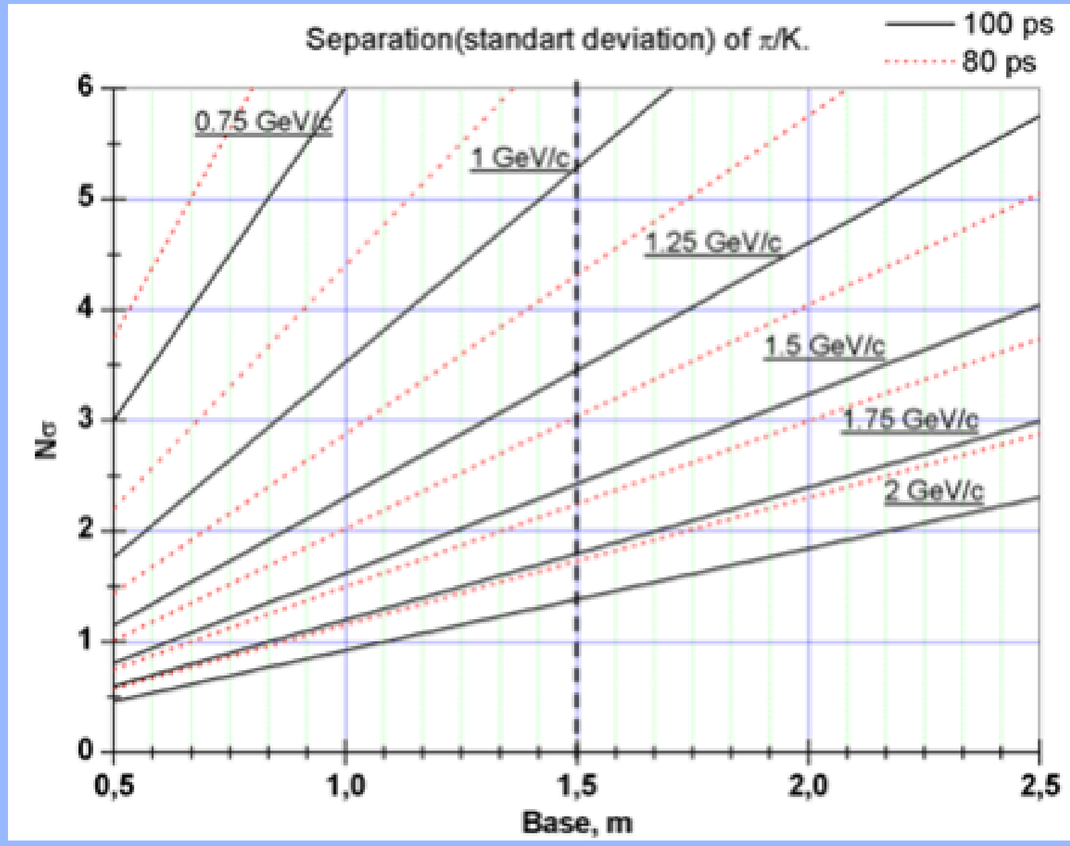

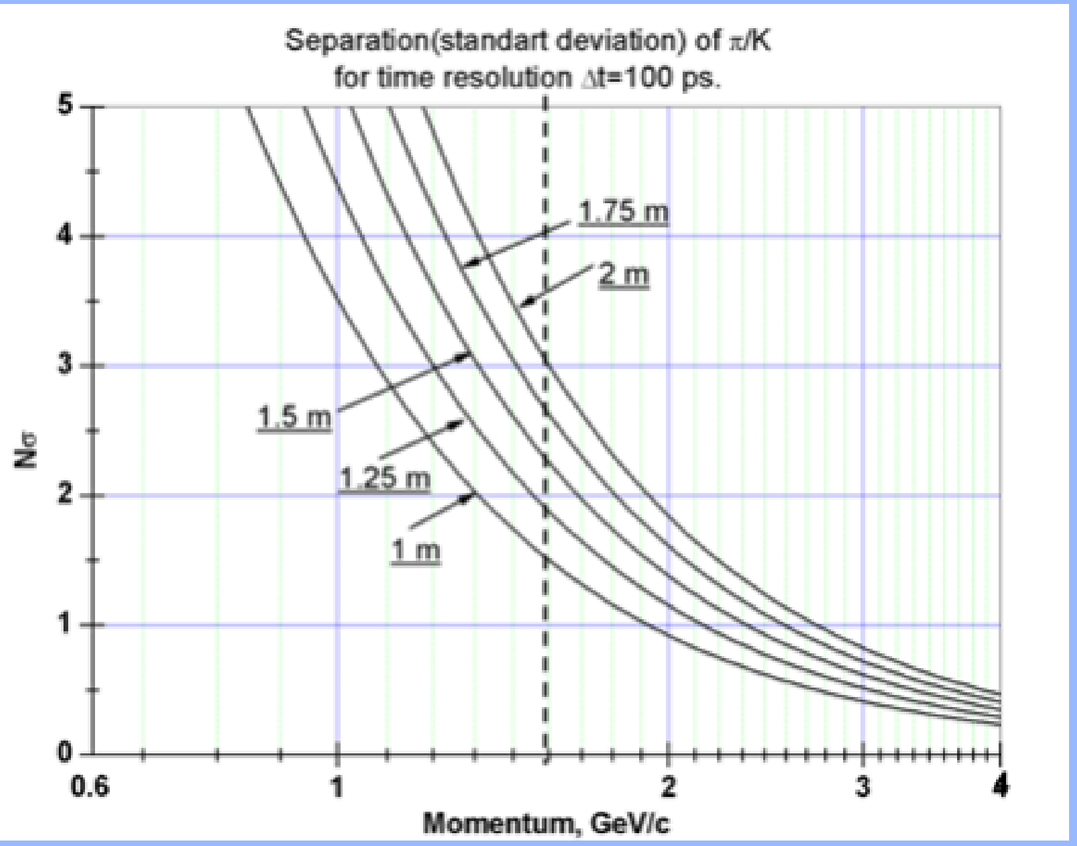

In Fig. 4 we present the fraction (in percent) of pions and kaons below a particular momentum as a function of momentum. These distributions are obtained for the particle spectra. One may conclude that TOF system can separate pions on the level of 99 % and kaons – almost 98 % up to the total momentum of 1.5 GeV/c.

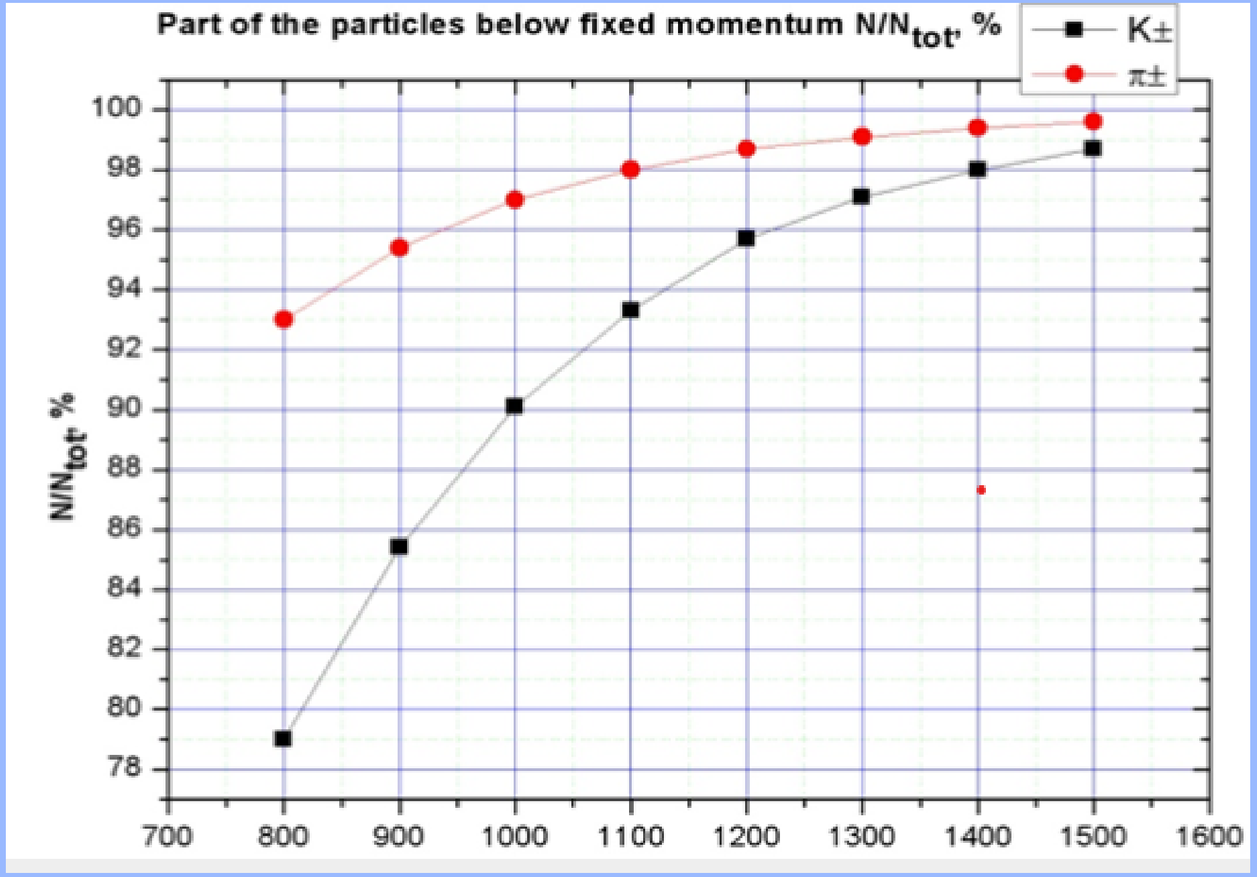

Figure: Part of the pions and kaons below a particular momentum (√(SNN)= 9 GeV).

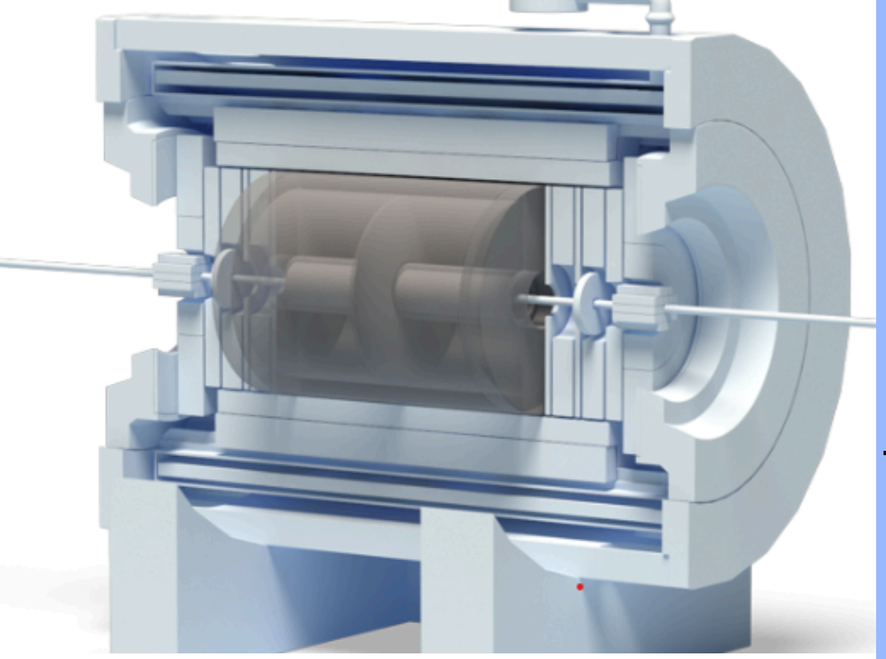

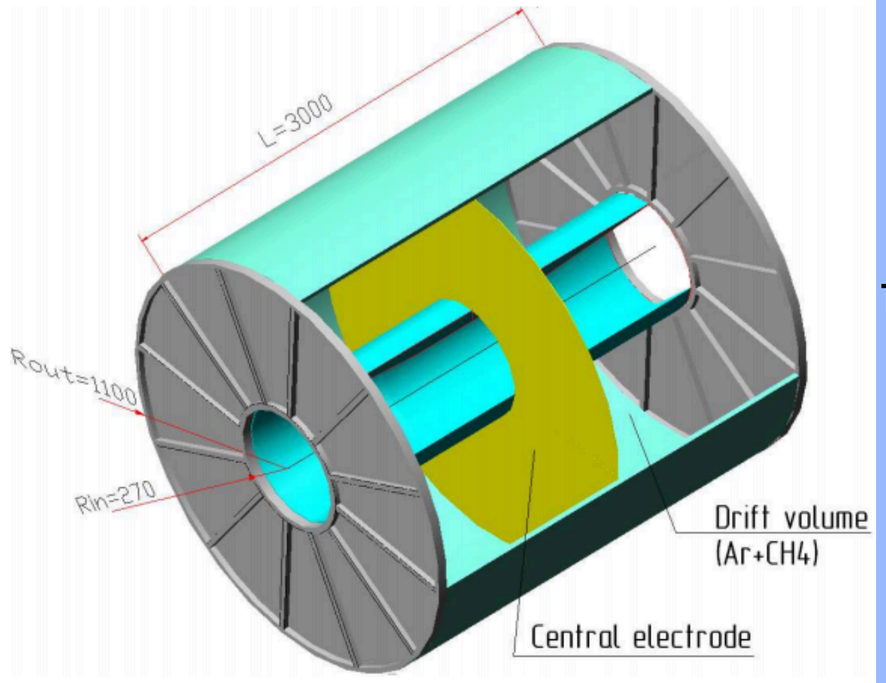

Fig. 1: Schematic view of the MPD TPC

Time projection chamber

The MPD time projection chamber (TPC) is the main tracking detector of the central barrel and, together with the internal tracking system, time of flight system and electromagnetic calorimeter has to provide charged particles momentum measurement with sufficient resolution, particle identification and vertex determination, two track separation and dE/dx measurement for hadronic and leptonic observables at pseudorapidities $|\eta| < 1.2$ and $p_t > 100$ MeV/c.

The electromagnetic calorimeter will provide, in conjunction with the data from the TPC, reliable electron identification to study dielectron processes. TPC has to provide the high dE/dx resolution in the high multiplicity environment of a Au + Au central collision to identify electrons with an efficiency of over 90% and reject pions at the level of 103.

The track reconstruction in the region of pseudorapidity beyond 1.2 is provided by both TPC and End cap straw tracker. In order to have excellent momentum resolution and identification capability in this region the end plate elements of the TPC and readout electronics which is mounted on them have to be minimized for material budget. Thus material budget of endplate and readout electronics is about 15%. The requirements to the TPC performance following from the physics described above are as follows:

— provide efficient tracking up to pseudorapidity region $|\eta| = 1.2$.

— the momentum resolution for charge particles about 2% at the transverse momentum of 300 Mev/c.<.p>

— the two-track resolution has to be about 1 cm in order to provide interference measurements with a resolution in relative momentum of a few MeV/c.

— for hadron and lepton identification a dE/dx resolution better than 8% is desirable

Zero degree calorimeter tracker

The events classification by centrality of the relativistic nuclei collisions is a key topic of the experiments studying a strongly excited (hot and/or dense) hadronic matter properties. Obviously, the selection of central events is a necessary to study the most excited nuclear matter. However centrality classification not only separates central and peripheral events. Observables analysis in different centrality intervals appears very informative and allows to study space–time picture of the nuclear–nuclear collisions as well as hadronic matter properties, both of which impossible without centrality data involving. The importance of centrality classification can be illustrated by the following examples:

• The ratio of the elliptic flow to the space excentricity of the collision region is a constant for a wide range of the impact parameter, as it obtained at the RHIC experiments [273]. This fact as well as a great value of elliptic flow is a strong experimental indication for a small (≤ 1fm/c) thermalization time value. Such measurements are impossible without centrality classification of events, because space excentricity of the collision region is determined by centrality.

• For description of the Jet Quenching and J/Ψ suppression in nuclei–nuclei collisions the nuclear modification factor (RAA) is used. This factor depend from the number of binary collisions, which is determined by centrality.

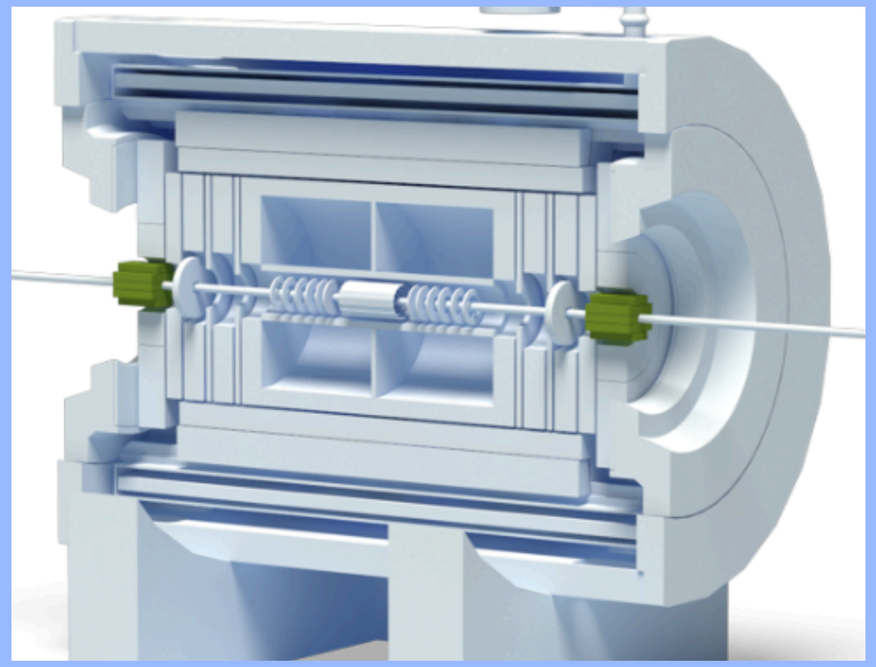

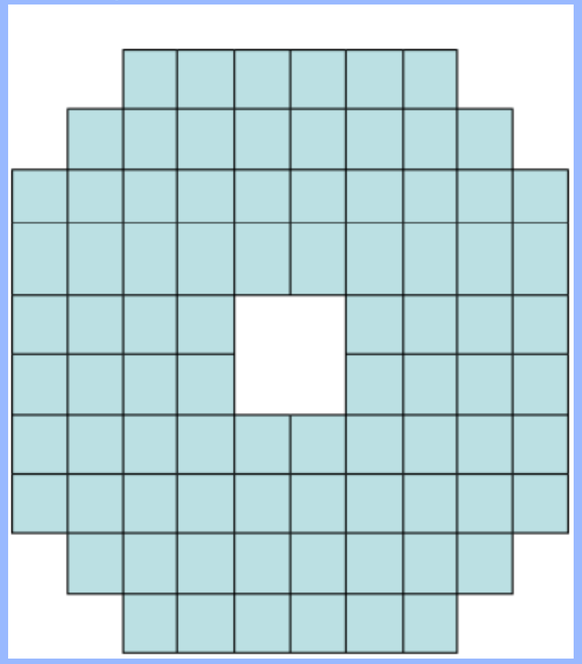

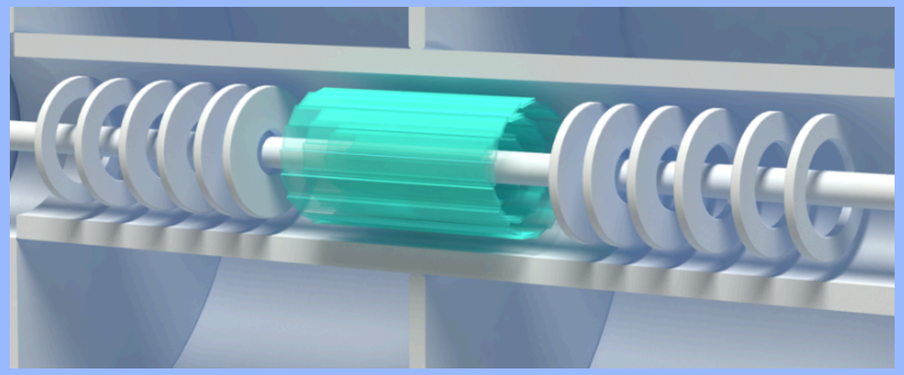

The "IT Tracker" refers to the Inner Tracker in the context of particle detectors used in high-energy physics experiments. This detection system is designed to track and measure the trajectories of charged particles passing through the detector in the closest region to the interaction point of nuclear collisions.
The Inner Tracker typically consists of a series of layers of high-precision detectors located near the interaction point, surrounding the area where nuclear collisions occur. These detectors are designed to record the position and direction of charged particles produced in collisions, allowing for the accurate reconstruction of these particles' trajectories.
The Inner Tracker is crucial for particle identification and event reconstruction in particle physics experiments, as it provides detailed information about the trajectories of particles produced in nuclear collisions. This enables researchers to study particle properties, identify new particles, and gain a better understanding of the physical processes occurring inside nuclear collisions.

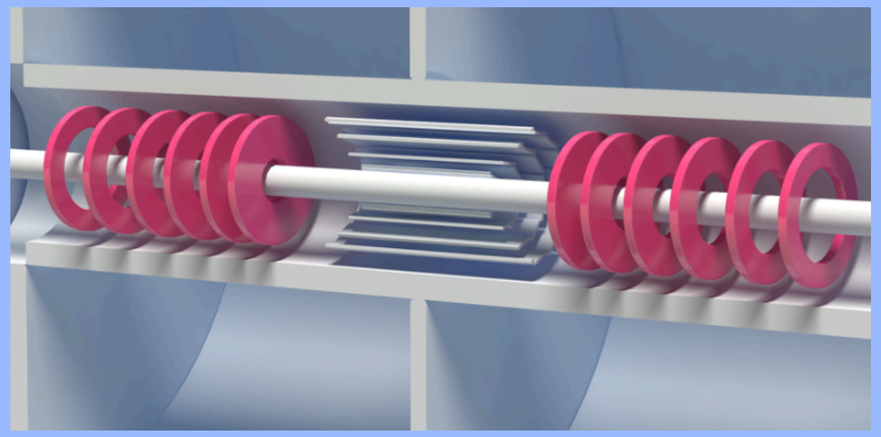

The "GEM Tracker" refers to the Gas Electron Multiplier (GEM) Tracker, a type of particle tracking system used in high-energy physics experiments. GEM trackers are composed of layers of gas detectors known as GEM foils, which are designed to detect and track charged particles produced in collisions.
GEM trackers utilize a principle called gas amplification to detect charged particles. When a charged particle passes through the gas in the GEM foil, it ionizes the gas atoms, creating free electrons. These electrons are then accelerated through a strong electric field, causing them to collide with other gas atoms and create additional electron-ion pairs. This process results in a cascade of electrons, leading to a significant amplification of the signal, which can be detected and used to determine the trajectory of the original charged particle.

Mini Bebe

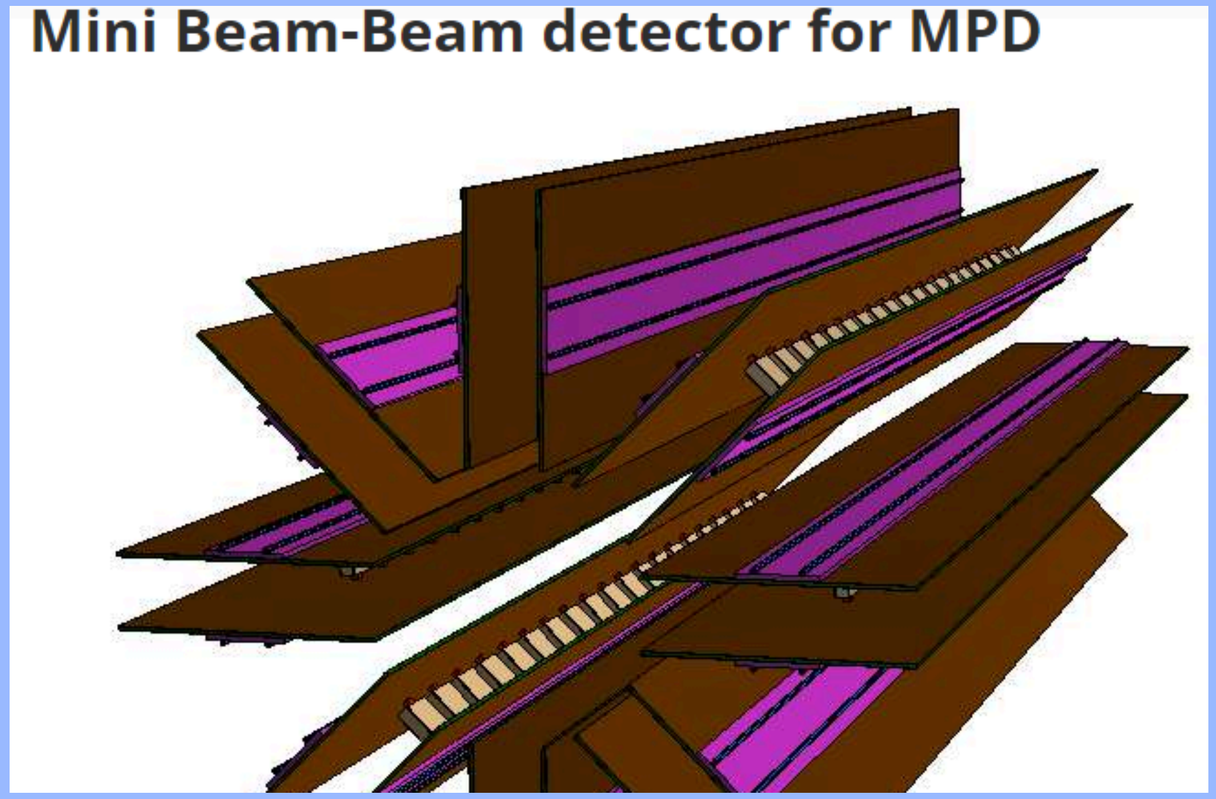

The ongoing construction of the MPD experiment at the NICA facility in JINR is focused on exploring the properties of matter under extreme conditions of temperature and density. This apparatus comprises various subdetectors (ITS, TPC, TOF FHCAl, ECal, and FFD), to be installed in two phases. Additionally, there are plans for extra detectors, notably the mini Beam Beam detector (miniBeBe), primarily designed as a level-0 trigger for the TOF detector. Evaluating the miniBeBe's performance is crucial to support its proposal. The primary objective of this interest project is to understand detector development, analyze multiplicity distributions, and assess the potential of MiniBeBe to aid in determining the centrality of heavy ion collisions.

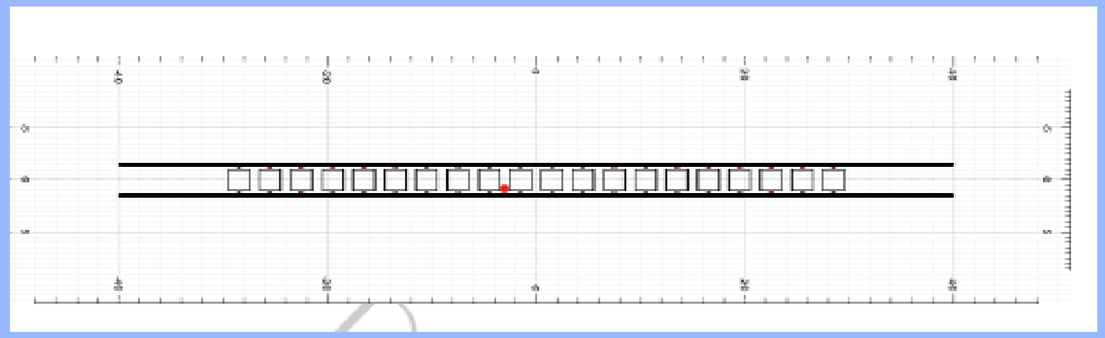

(a) Position of the 20 plastic scintillators along the rail

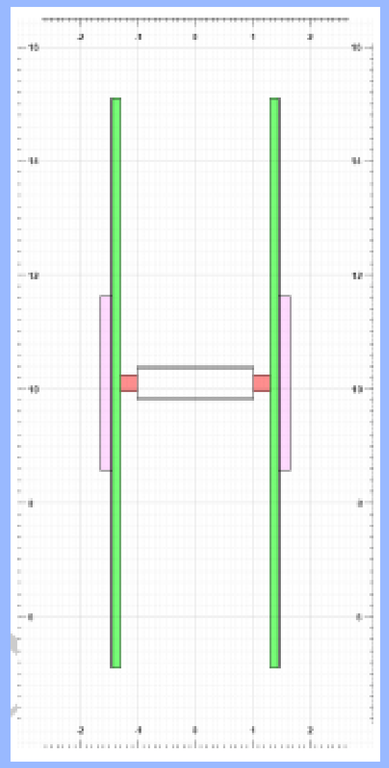

(b) Profile of the H-shaped rail. In the drawing appears
the SiPMs in red at each side of the plastic, and the Hshape formed by the PCB on green and the cooling plates
in pink

This inner beam counter detector aims primarily to deliver a rapid activation trigger for the MPD's Time-Of-Flight (TOF) detector during events with low particle multiplicity.

• It comprises 20 square plastic scintillator cells measuring 20x20x3 mm^3 each, along with 1,280 SiPMs covering an effective sensitive area of 128,000 mm^2.

• The detector is housed in a cylindrical structure with a length of 60 cm.

• It has an inner diameter of 25 cm and an outer diameter of 27 cm.

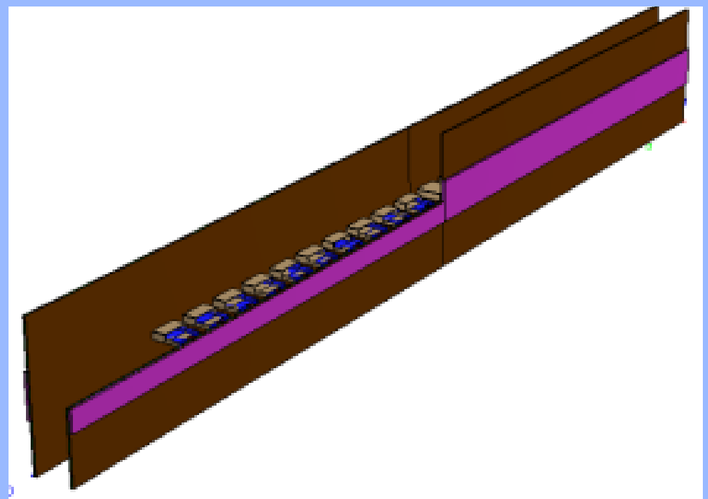

(c) Schematic view of the rail

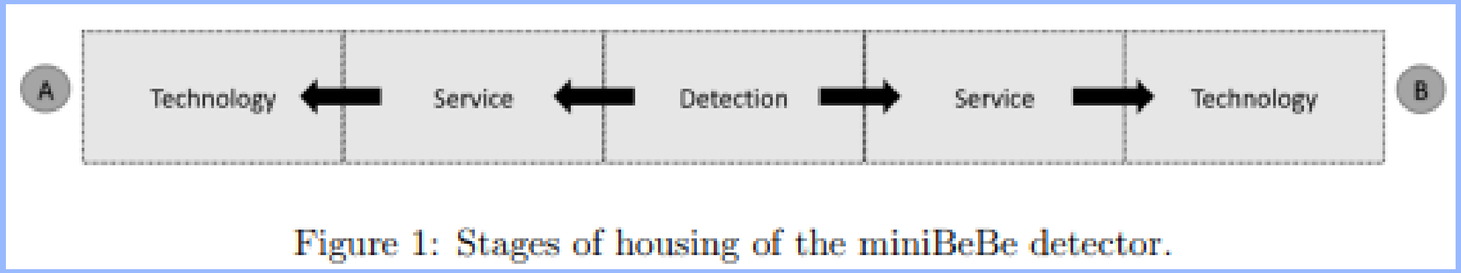

Figure 1: Stages of housing of the miniBeBe detector.

Figure 1:

- Depicts the stages of the miniBeBe detector.
- Notable are two distinct sides labeled as A and B, reflecting the adaptation of the miniBeBe detector to the ITS detector's general housing
- The A-side connects to the supports of the 5th electronic layer of the ITS detector, while the B-side connects to the supports of the 4th layer

Design Stages of Housing for MiniBeBe Detector

Detection Stage:
Located in the central part of the housing.
Contains scintillating plastic and SiPMs positioned within the ion collision range.

Service Stage:
Houses the "Front end" boards responsible for converting analog signals to digital.
Includes pipes, cables, and cooling system power sources.

Technology Stage:
Facilitates connections to extract signals from the housing and route them to the MPD detector rack.

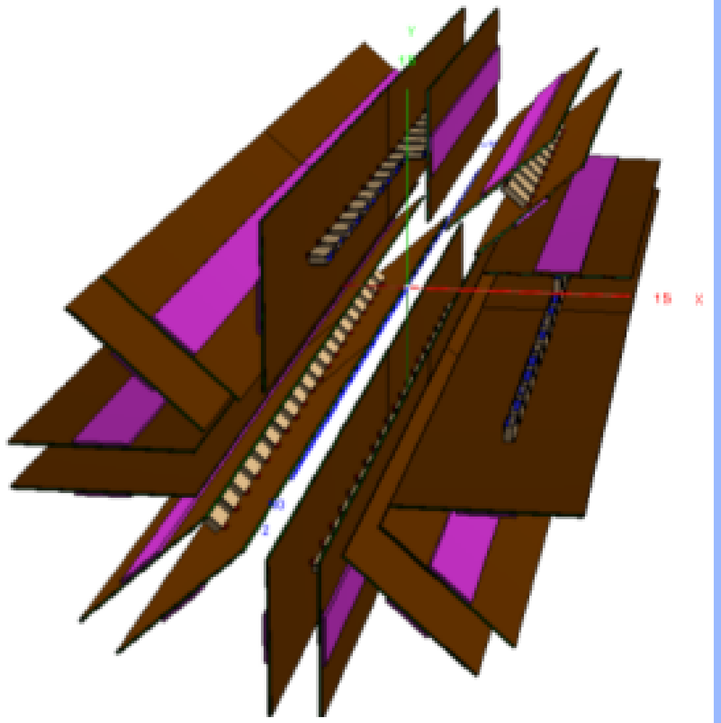

(a) perspective view

Trigger Efficiency of MiniBeBe

Primary Vertex Position Range: (-40, 40) cm Near 100 cm

Detection Probability:

Rings near the primary vertex:

Low Cut: 2% - 5%

Vertex near 100 cm: ~1%

Strong Cut:

Near the origin: 1% - 3.4%

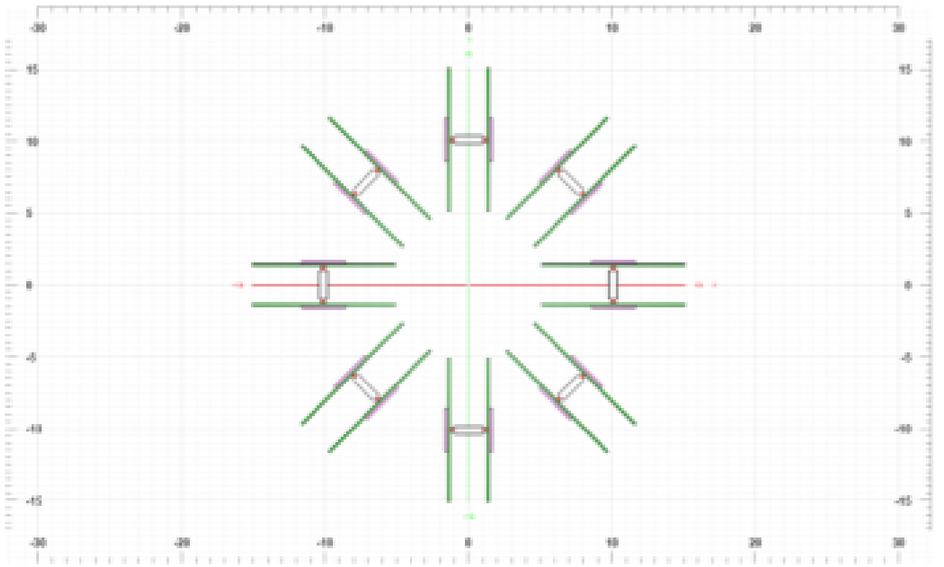

(b) Top view of the arrange of rails in which is possible appreciate the free space for the beam pipe.

Figure 2: Schematic view of MiniBeBe formed by 8 H-shaped rails.

Trigger Efficiency:

Primary vertex near zvtx ∈ (-50, 50) cm:

20% for both cases Up to 50% for low cut in events near the origin

Collision Systems:

Bi + Bi System:

√sNN = 9.2GeV

Energy deposited in each ring similar to the pp case

Impact of Primary Vertex Displacement:

Probability of detecting at least one charged particle in each ring as a function of the impact parameter.

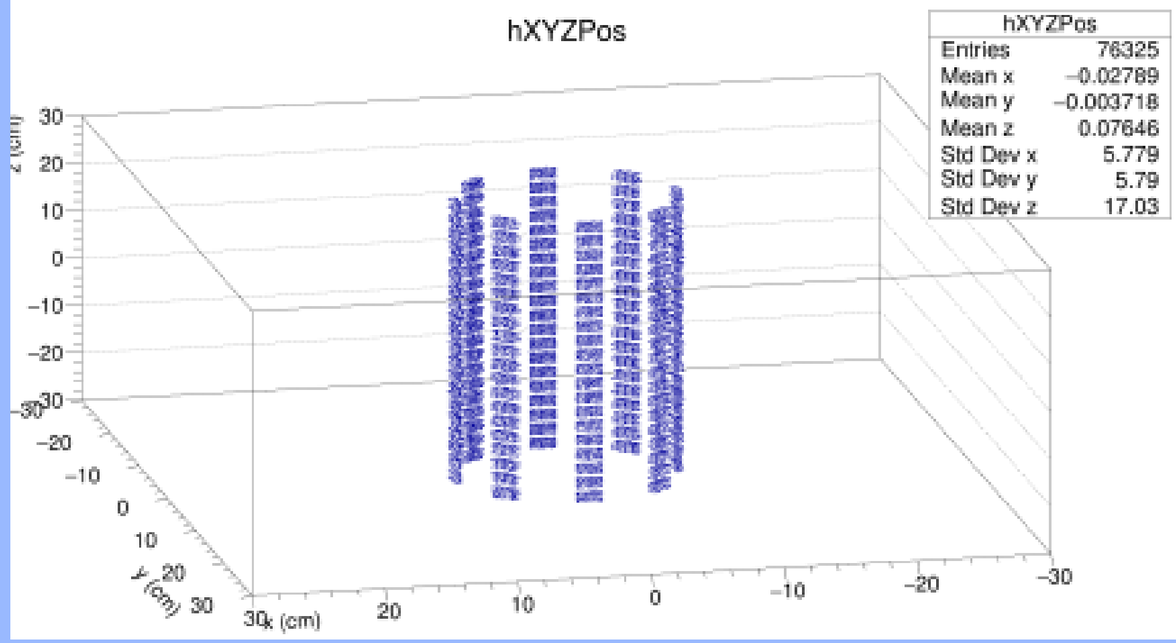

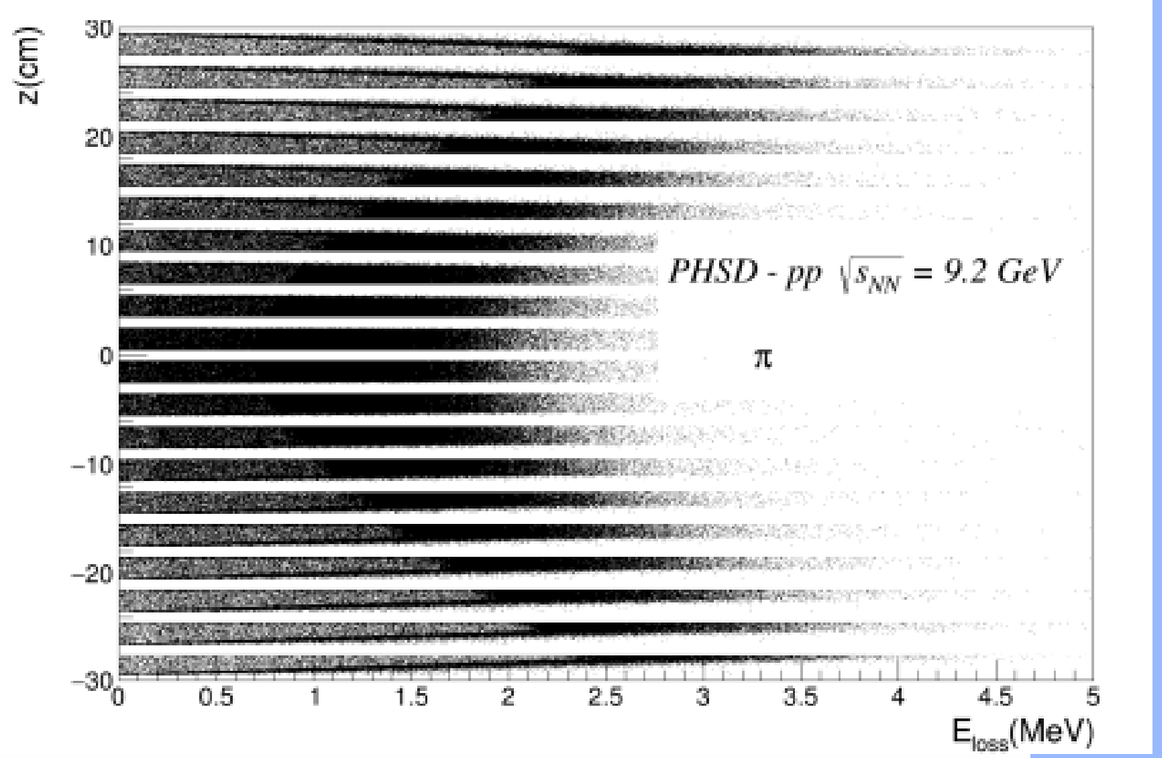

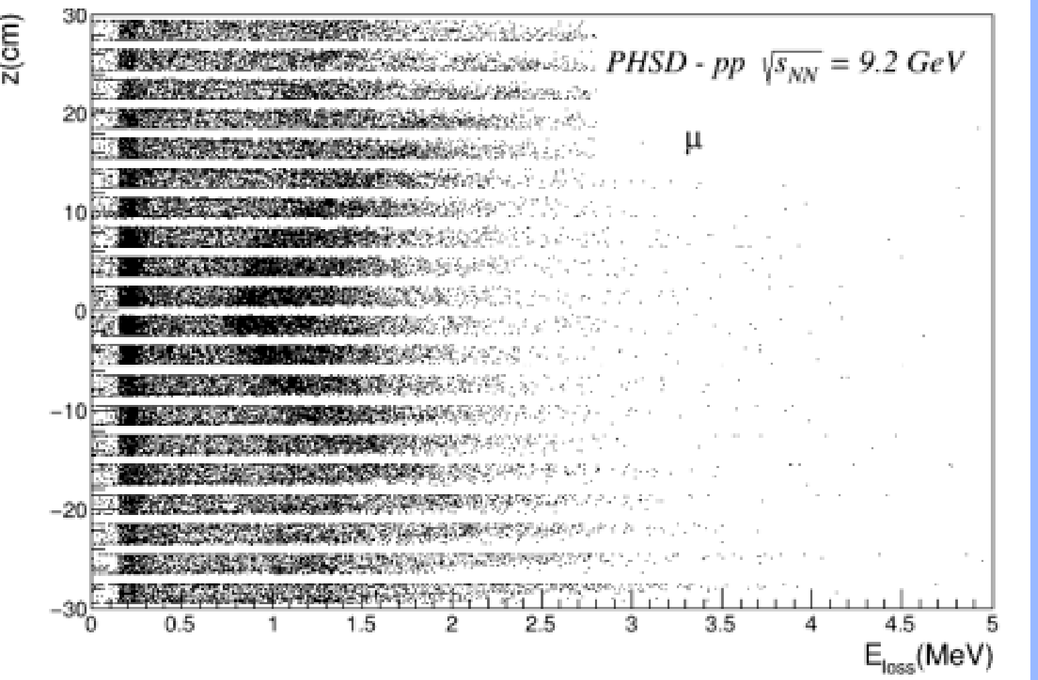

Figure up: Energy loss for π (upper pannel) and μ (lower panel). In both cases there are particles that does
not cross the full lenght of plastic scintillator, and in the case of muons there is a noise at 0.2 MeV
figure down

The trigger efficiency as a function of the impact parameter is shown in the figure 14. The efficiency is close to 1 for b < 12 fm and higher than 90% for b < 14fm. Further analysis will be done with other collision

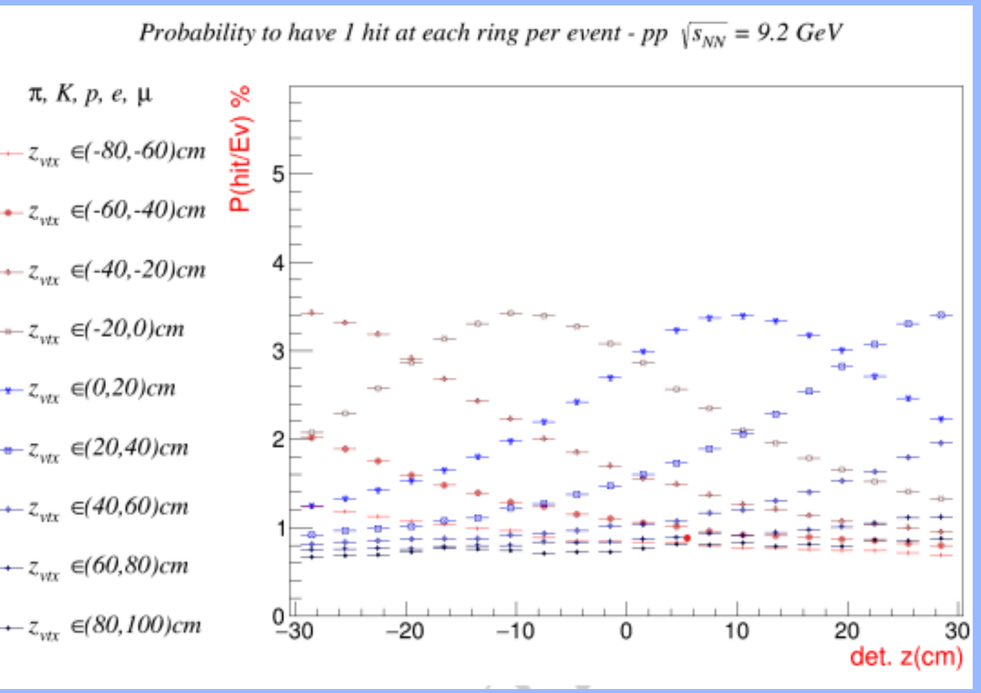

Figure : Probability to have at least one hit per event at each ring. Assuming particles with deposition of energy higher than Eth > 0.892MeV.

Material Budget:

- Radiation length is utilized to determine the thickness of a detector.
- The detector thickness in units of X0 is referred to as the material budget.
- The material traversed by a particle depends on the primary vertex position and the crossing angle.
- We model the materials in the rail with simple geometric volumes.
- Both SiPMs and scintillators use the same material for simulation.
- Scintillators are coated with 0.5 mm thick mylar.
- PCBs consist of FR-4 material between two layers of 0.1 mm thick copper.
- For the cooling system, we assume a carbon fiber sheet measuring 800 mm x 30.6 mm x 2 mm and two water pipes with a radius of 1.025 mm for each plate.

- The average contribution to the material budget of MiniBeBe is shown in Table 1.
- The highest contribution comes from the copper layers in the PCBs, nearly 7%.
- We scan the radiation length of MiniBeBe using a box generator with Geantino.
- In the simulation, we include the cave, pipe, magnet, cradle, and MiniBeBe to avoid shadows.
- The effective radiation length is approximately 1-2% in all projections.
- Figure 19 depicts the radiation length for different detectors as a function of η.

Design of Electronic Support:

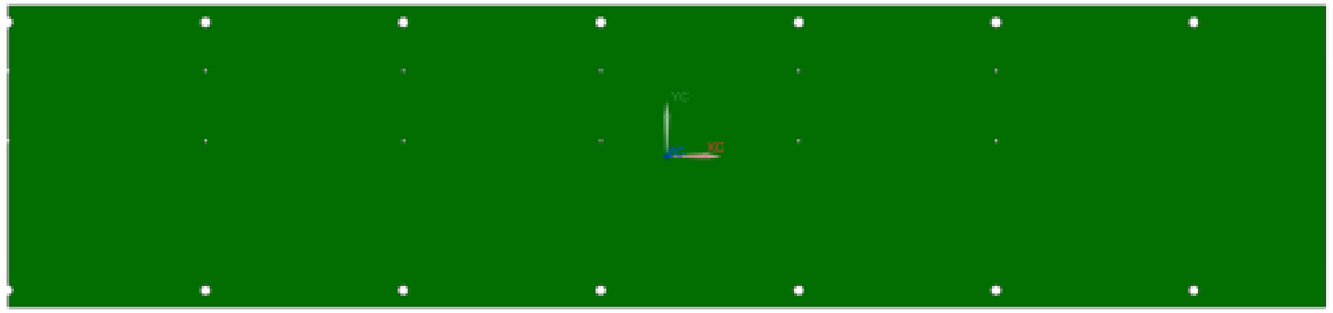

Figure 2: Electronic Board to construct module, 400mm

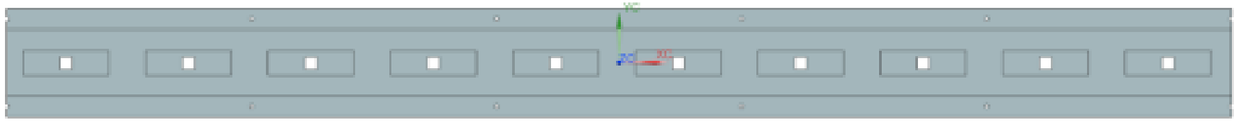

Figure 3: Frontal view of SiPM suport

Figure 3 shows the rear view of the support, where every 30 mm there is a window to place SiPM.

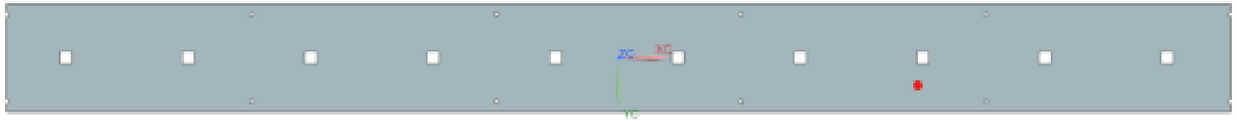

Figure 4: Back view of SiPM suport

- The total length of the electronic boards will be 800mm. However, for manufacturing reasons, the decision was made to manufacture two pieces of 400mm each, which will later be joined.
- There will be two signal outputs or connectors, one on each side of the electronic module, corresponding to each half of the boards.
- In Figure 2, the prototype electronic board with a length of 400mm, a width of 90mm, and a thickness of 1.6mm is observed.
- Perforations will be used for fastening between electronic cards to assemble the electronic module.

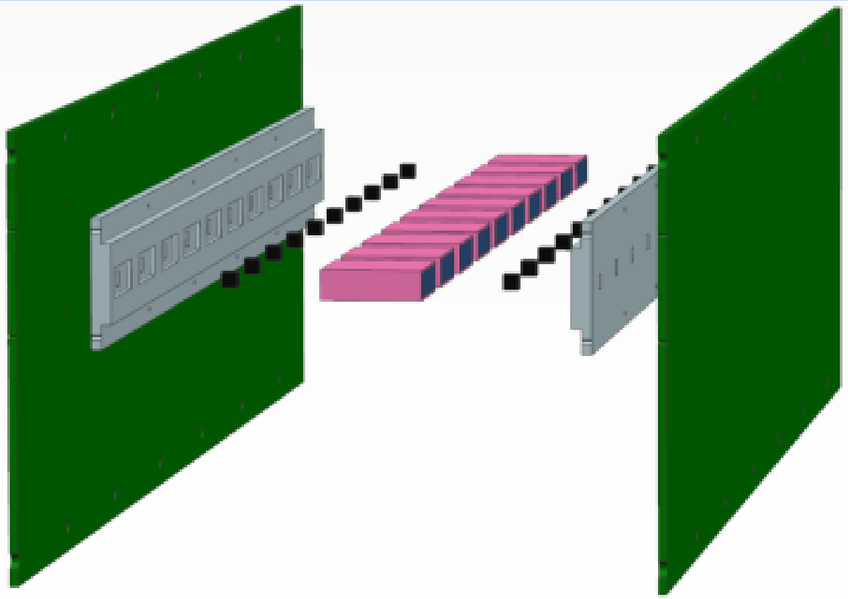

Figure 7: Explosion view of the electronic module assembly

In Figure 7, you can see all the components that are necessary to carry out the assembly of the electronic
module: scintillating plastic, SiPM, Mylar, SiPM support, electronic board. In the view half an electronic
module is observed, which corresponds to 400mm. At the end of the electronic board there is a free area
that will be used to place the connectors; in case there is not enough space for it, it is proposed to solder
the cables directly to the board to effectively use the available space

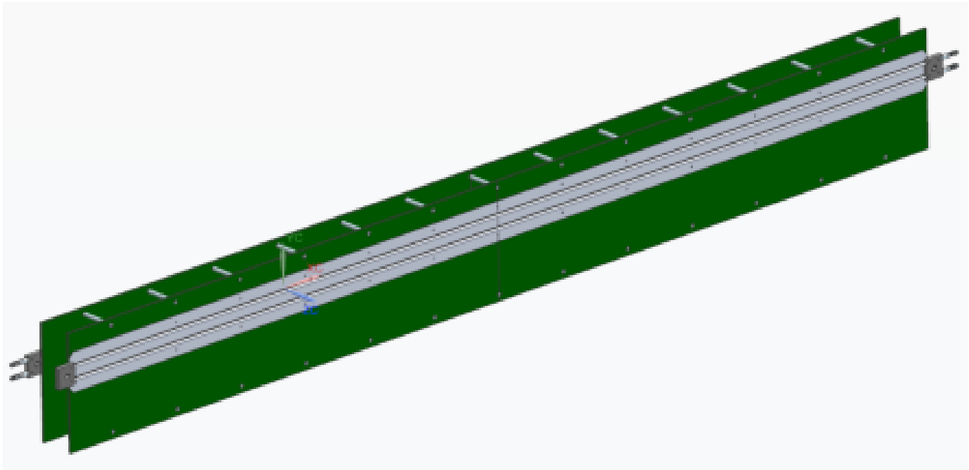

Figure 10: Isometric view of electronic module assembly with cold plate system

Figure 10 shows a fully assembled electronic module 800 mm long, including the cold plate system. The
fixing screws of the module are placed every 60 mm avoiding interfering in the detection area of scintillating
plastics. The cooling plate is also placed at a distance of 15mm from the center so that it is aligned with
the SiPMs, as these are the elements that need to be thermally stabilized.

Integration of miniBeBe detector to the ITS detector housing

The way the miniBeBe detector is placed inside the outer barrel of the ITS detector is with the replacement of the flange of the 4th layer of the ITS detector by the support flange of the miniBeBe detector, both have 12
the same dimensions. Therefore, the flanges of the miniBeBe detector is connected and supported by the flanges of the 5th layer of the ITS detector.

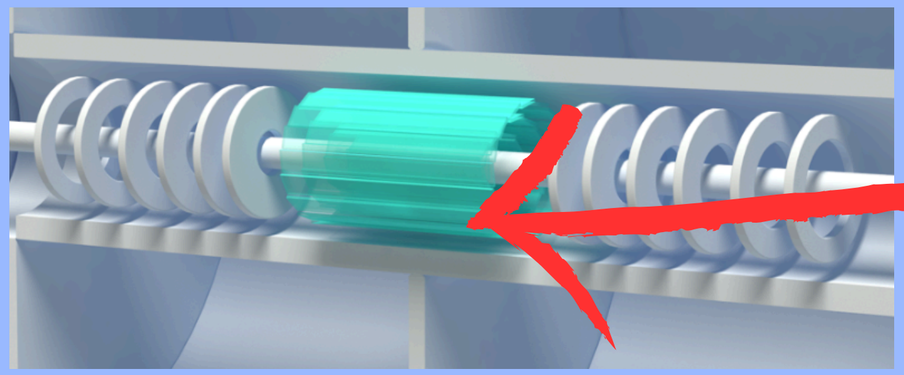

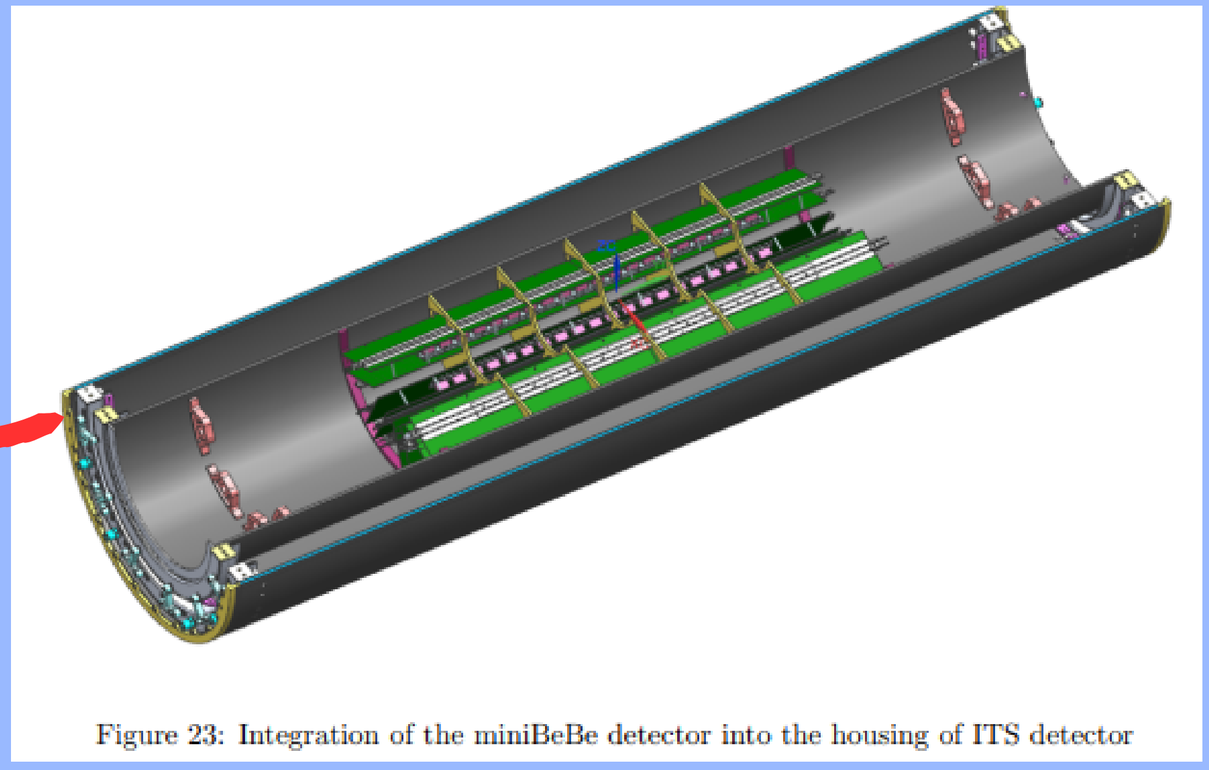

Figure 23: Integration of the miniBeBe detector into the housing of ITS detector

Readout Electronics System for FFD and TOF Detectors

"PRESENTATION BASED ON THE CONFIGURATION AND OPERATION OF READOUT SYSTEMS FOR PARTICLE DETECTORS.

JESUS ARMANDO CERNA

IMPORTANCE OF READOUT OF ELTRONICS IN FFD

ACCURATE DATA ACQUISITION:

THE READOUT ELECTRONICS OF THE FFD IS RESPONSIBLE FOR CAPTURING AND RECORDING SIGNALS GENERATED BY DETECTED PARTICLES. IT ENSURES THAT COLLECTED DATA IS PRECISE AND RELIABLE, WHICH IS FUNDAMENTAL FOR THE SUCCESS OF SCIENTIFIC EXPERIMENTS.

PARTICLE IDENTIFICATION:

PROPER READING OF SIGNALS DETECTED BY THE FFD ALLOWS FOR THE IDENTIFICATION AND CLASSIFICATION OF INTERACTING PARTICLES. THIS IS ESSENTIAL FOR UNDERSTANDING THE NATURE OF PARTICLES AND THE UNDERLYING PHYSICAL PROCESSES.

MEASUREMENT OF PHYSICAL PARAMETERS:

THE FFD'S READOUT ELECTRONICS FACILITATES THE MEASUREMENT OF VARIOUS PHYSICAL PARAMETERS OF DETECTED PARTICLES, SUCH AS ARRIVAL TIME, DEPOSITED ENERGY, AND IMPACT POSITION. THESE DATA ARE CRUCIAL FOR CONDUCTING DETAILED ANALYSES OF COLLISION EVENTS.

DETECTOR CONTROL AND MONITORING:

THE READOUT ELECTRONICS ALSO PLAY A SIGNIFICANT ROLE IN THE CONTINUOUS CONTROL AND MONITORING OF THE DETECTOR. IT ALLOWS FOR ADJUSTING DETECTOR OPERATION PARAMETERS, PERFORMING PERIODIC CALIBRATIONS, AND DIAGNOSING POTENTIAL OPERATIONAL ISSUES.

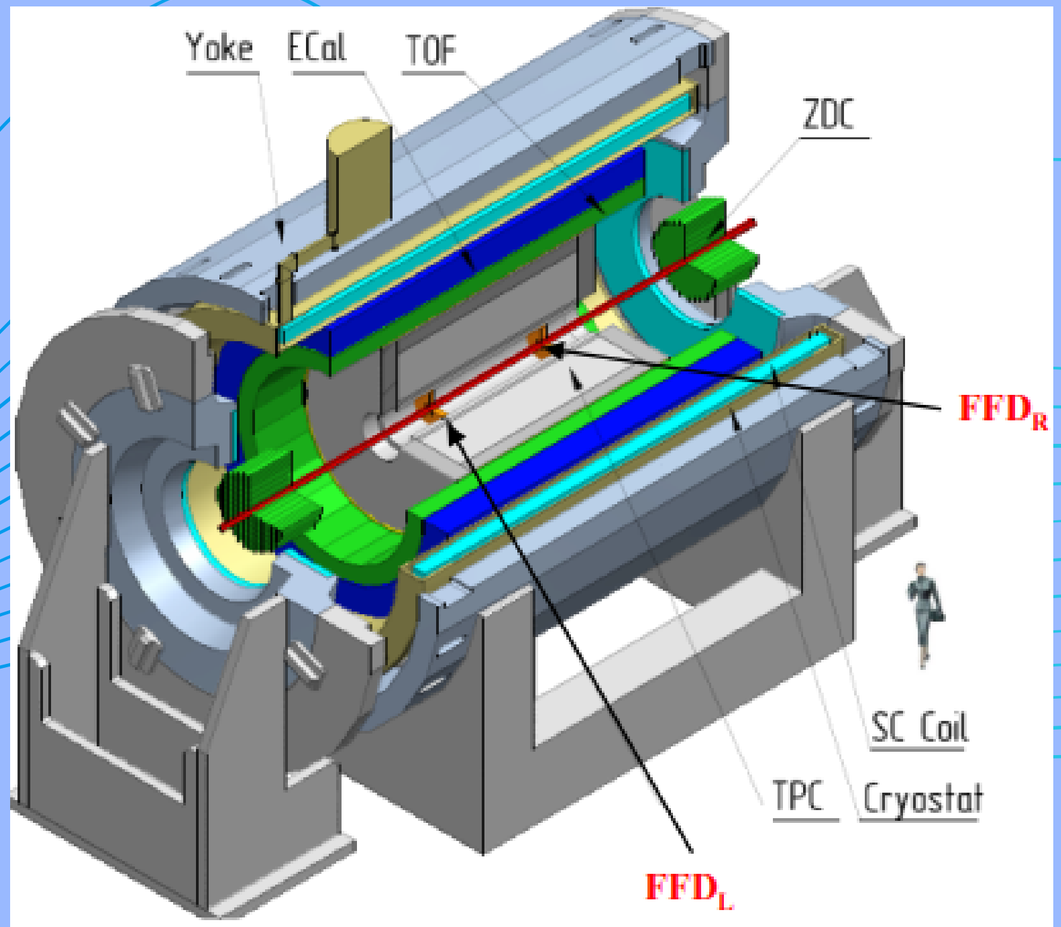

FFD layout in the MPD setup

FFD arrays

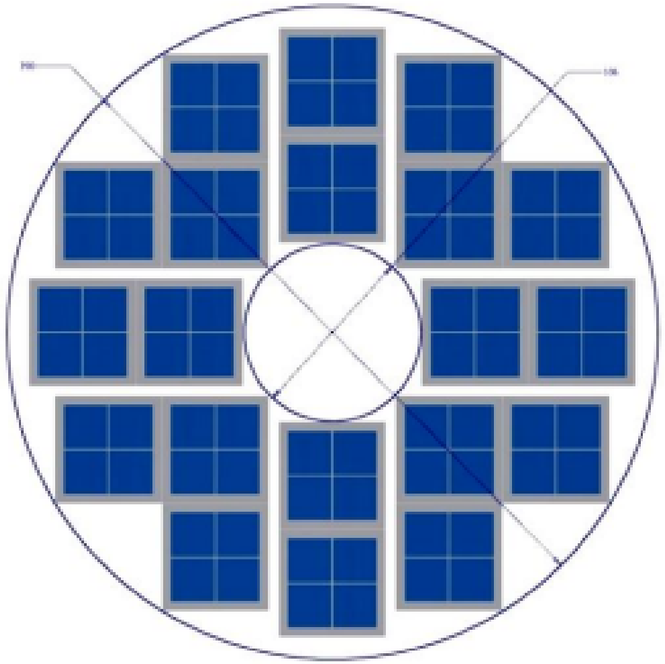

Number of arrays	2
Number of modules	20 × 2
Number of channels	80 × 2
Required time resolution, σ	< 50 ps
Operation in magnetic field, B	0.5 T

LOCATION: THE FFD IS TYPICALLY PLACED NEAR THE MAIN INTERACTION POINT IN A PARTICLE COLLIDER EXPERIMENT TO DETECT CHARGED PARTICLES OR PHOTONS EMERGING FROM THE INTERACTION REGION.

PRIMARY FUNCTION:

ITS PRIMARY FUNCTION IS TO DETECT AND RECORD THE PRIMARY PARTICLES PRODUCED IN COLLISIONS AND PROVIDE INFORMATION ABOUT THEIR TRAJECTORY, ENERGY, AND OTHER IMPORTANT PARAMETERS.

CONFIGURATION AND ELECTRONIC CONNECTIONS:

THE FFD IS EQUIPPED WITH A READOUT ELECTRONICS SYSTEM THAT INCLUDES TDC72VHL MODULES FOR MULTI-HIT TIME STAMPING AND CAEN MOD. N6742 DIGITIZERS FOR SIGNAL DIGITIZATION. THIS READOUT ELECTRONICS SYSTEM IS RESPONSIBLE FOR ACQUIRING, PROCESSING, AND STORING THE DATA COLLECTED BY THE FFD.

CALIBRATION AND CONTROL:

THE FFD REQUIRES PERIODIC CALIBRATION AND ADJUSTMENT TO ENSURE ITS PROPER OPERATION. THIS INVOLVES THE USE OF CALIBRATION PULSES AND PROPER CONFIGURATION OF READING AND DATA PROCESSING PARAMETERS.

TIME-TO-DIGITAL CONVERTER TDC72VHL

2-CHANNEL TIME-TO-DIGITAL CONVERTERS (TDC72VHL) BASED ON THE HPTDC CHIP [5] WERE DEVELOPED AND PRODUCED FOR DIGITIZATION OF LVDS SIGNALS AND DATA ACQUISITION (FIG. 4). FIRST EXPERIMENTS ON THE MRPC TIME RESOLUTION EVALUATION IN 2012 SHOWED THAT LARGE INTEGRAL

NONLINEARITY (FIG.4) OCCURS WITH TDC THAT OPERATS IN THE MODE OF 24.4 PS PER BIN. THIS NONLINEARITY CAUSES STRONG DEGRADATION OF TIME DISTRIBUTION. THE CONTRIBUTION OF THIS NONLINEARITY
AND THE METHOD TO ELIMINATE IT HAS ALREADY BEEN SHOWN IN THE HPTDC MANUAL AS WELL AS IN OTHER PUBLICATIONS.

FIG. 4. VIEW OF THE TDC72VHL MODULE.

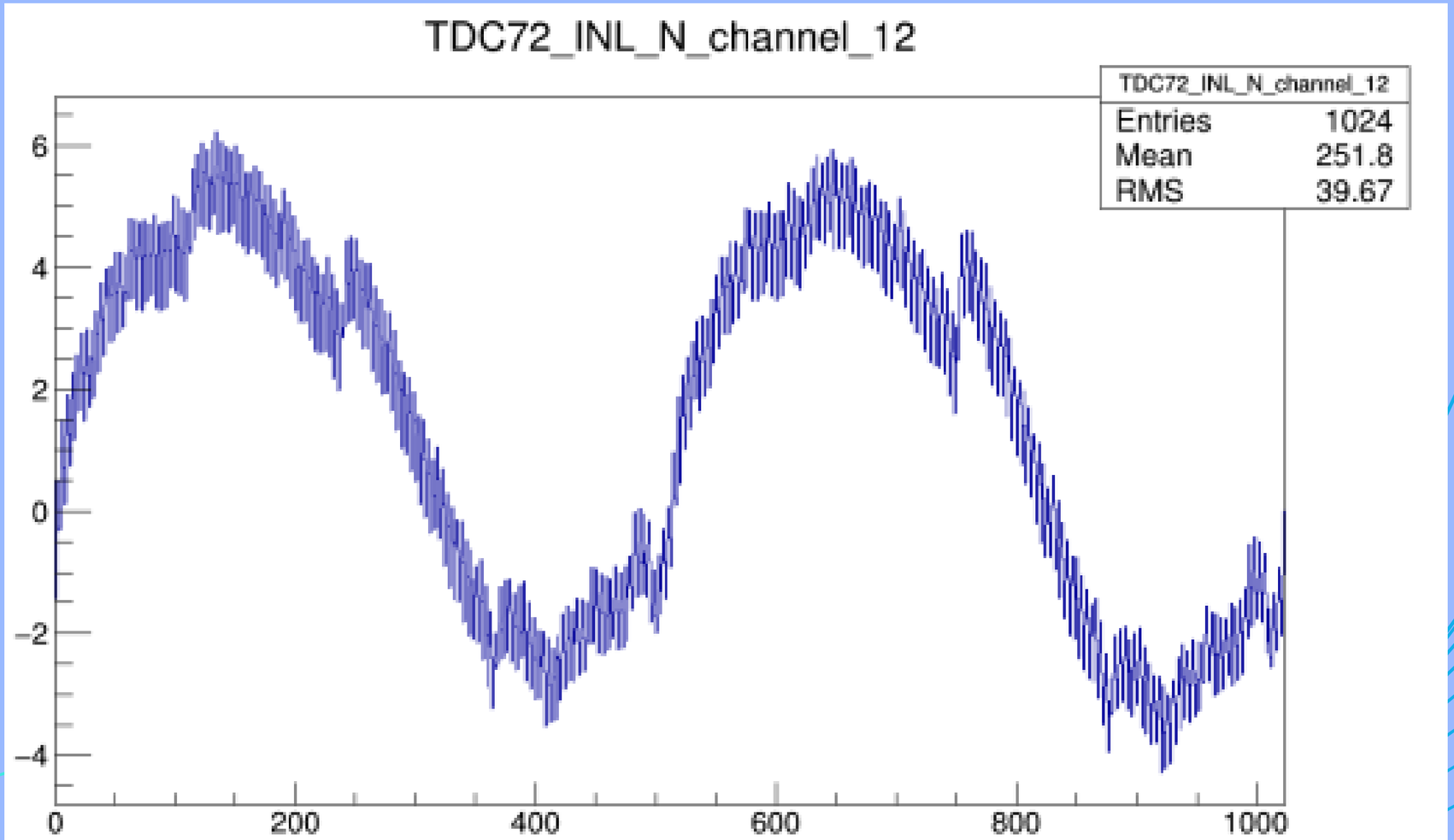

Fig. 5. Integral nonlinearity for one channel [bins].

REALIZATION AND METHODS

THE METHOD OF UNIFORM FILLING OF A TIME GAP WITH RANDOM EVENTS (CODE DENSITY TEST) WAS USED FOR CALIBRATION (CONSIDERATION OF NONLINEARITY) OF 16 VME TDC72VHL MODULES. A LARGE STATISTICS (~10 000 000 EVENTS PER CHANNEL) WAS COLLECTED TO MINIMIZE THE STATISTICAL ERROR (~1%).

SIGNAL FROM THE PHOTOMULTIPLIER WAS USED AS A TRIGGER SIGNAL. THE TRIGGER REACHED U40VE (UNIVERSAL 40 CHANNEL VME AND ETHERNET INTERFACE BOARD) AND THE FVME2 TRIGGER MODULE THROUGH WHICH INFORMATION WAS EXCHANGED WITH THE CLIENT (FIG. 6.). THE SELF-MADE LVDS GENERATOR (FIG.7.) WAS USED FOR UNIFORM FILLING OF A TIME GAP. THEN THE LVDS SIGNAL IS TRANSMITTED TO THE TDC72VHL MOLEX CONNECTOR. OUTPUT DATA ARE WRITTEN IN A BINARY FILE (~8 GB
FOR ONE TDC). THEN BINARY FILE WITH THE DATA WERE DECODED BY BMNROOT FOR FURTHER PROCESSING.

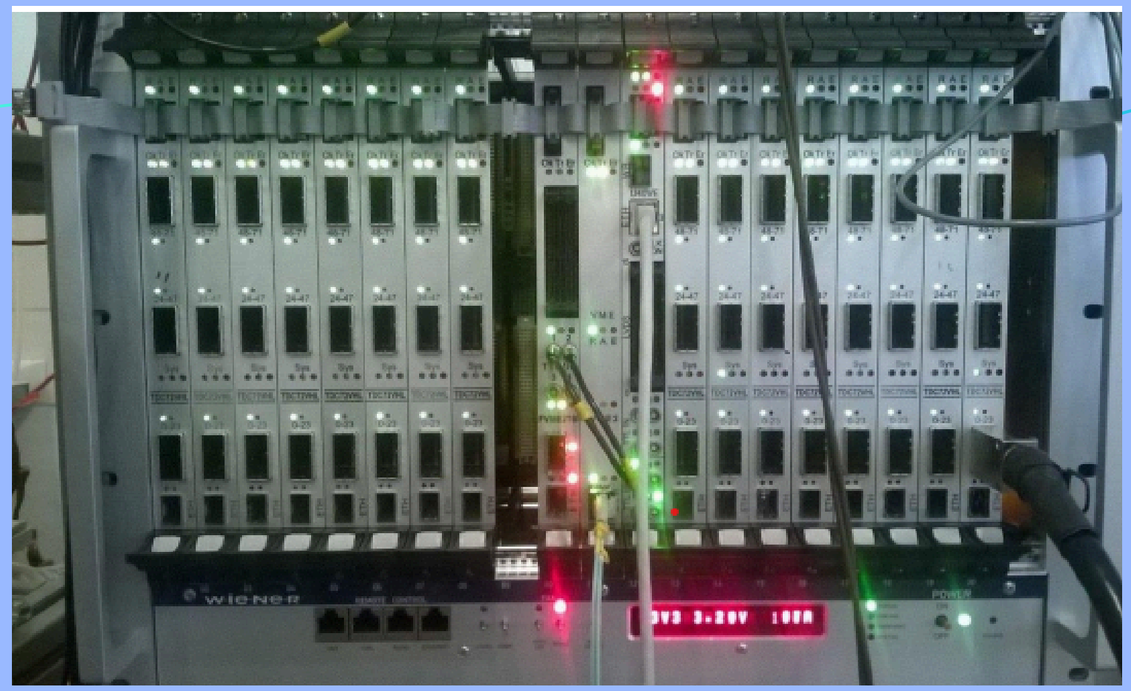

FIG. 6. VME CRATE WITH U40VE, FVME2 AND 16 TDC72VHL MODULES

FIG. 7. 72 CHANNELS LVDS GENERATOR

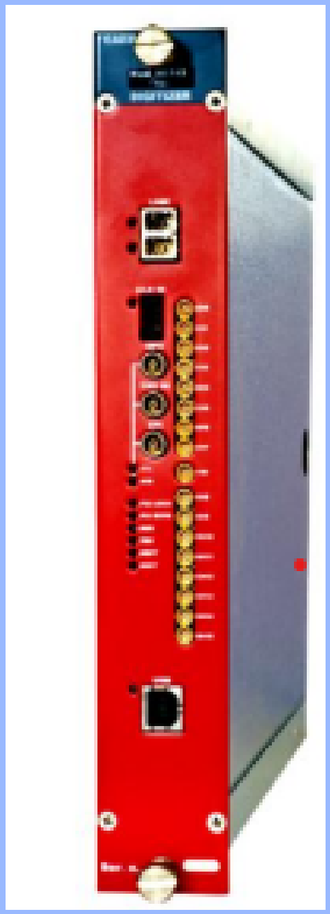

CAEN MOD. N6742 DIGITIZER

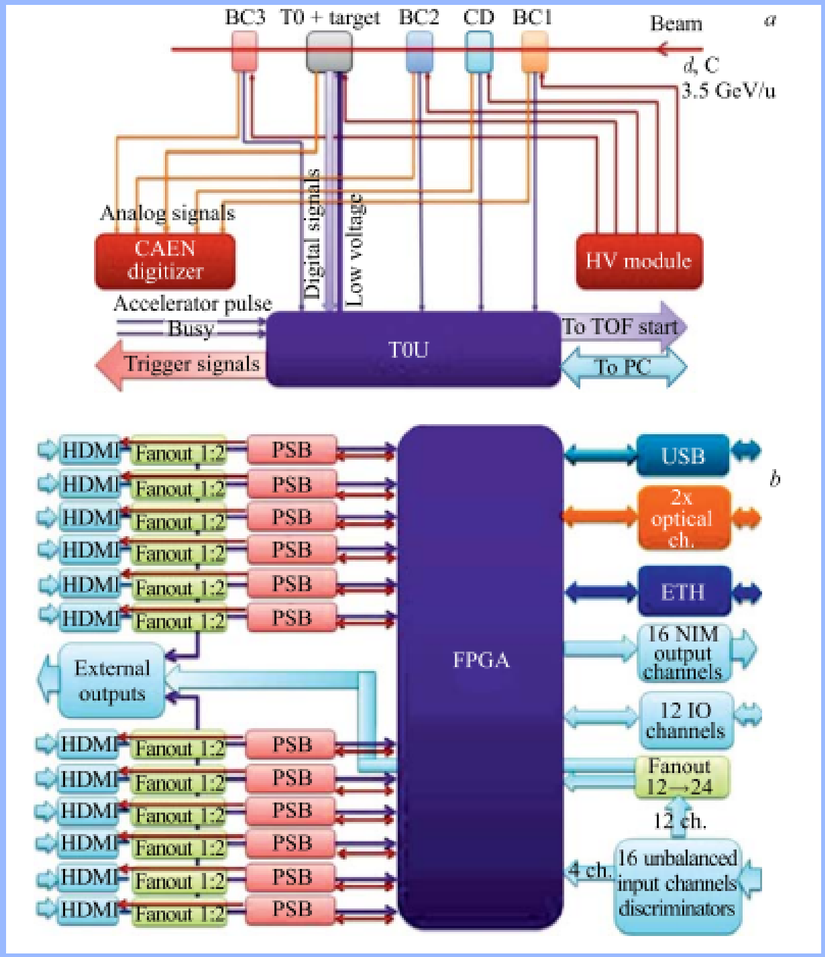

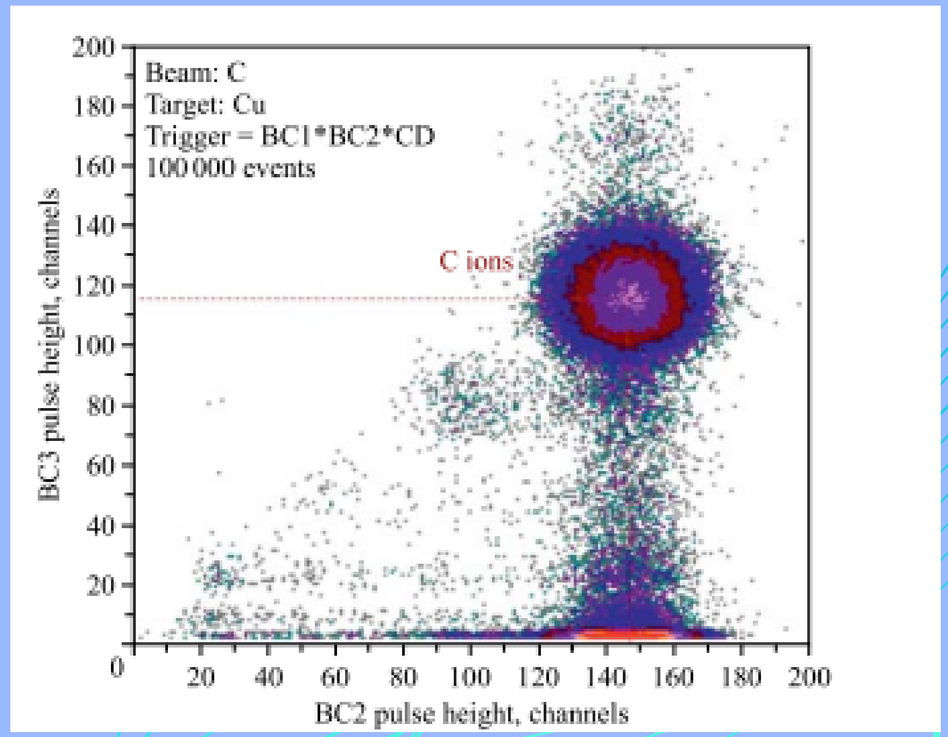

IN PARALLEL WITH GLOBAL RUNS, LOCAL RUNS WERE CARRIED OUT WITH BEAM AND T0 DETECTORS. HERE THE SIGNALS WERE FED TO 5-G/S DIGITIZER CAEN MOD. N6742. THE TIME RESOLUTION OF THE CD DETECTOR MEASURED WITH CAEN DIGITIZER WAS 85 PS FOR DEUTERON BEAM AND 27 PS FOR CARBON BEAM

CONCLUSION:

THE DESIGN AND OPERATION OF THE READOUT ELECTRONICS SYSTEM FOR FFD AND TOF DETECTORS ARE CRITICAL FOR ACQUIRING PRECISE DATA AND EFFECTIVELY CONTROLLING THE DETECTORS. BASED ON THE TDC72VHL FOR MULTI-HIT TIMESTAMPING, DEVELOPED AT THE JOINT INSTITUTE FOR NUCLEAR RESEARCH (JINR) HIGH ENERGY PHYSICS LABORATORY, THIS SYSTEM OFFERS A TEMPORAL RESOLUTION OF 25 PS. EACH FFD SUBDETECTOR HAS 80 LVDS LINES AND 2 CALIBRATION LINES, REQUIRING TWO TDC MODULES INSTALLED IN A NEARBY VME CRATE. THE LVDS SIGNALS ARE DIRECTED TO THE TDC INPUTS VIA MOLEX P/N 11102512XX CABLES WITH MOLEX 76105-0585 CONNECTORS.

LOCAL DATA ACQUISITION FOR FFD IS BASED ON CAEN MOD. N6742 DIGITIZERS WITH 16 INPUTS AT 5 GS/S. FOUR OF THESE MODULES ARE NECESSARY FOR ADJUSTING AND CONTROLLING THE DETECTORS. TO ACHIEVE THIS, THREE DIFFERENT TYPES OF PULSES FROM EACH FFD MODULE ARE DIRECTED TO THE DIGITIZER INPUTS: COMMON ANALOG PULSE, COMMON LOGICAL PULSE (NIM), AND ANALOG PULSE FROM ONE OF THE FOUR INDIVIDUAL FEE CHANNELS. THE DIGITIZER MODULES ARE HOUSED IN A NIM CRATE WITHIN THE SUBDETECTOR'S ELECTRONICS RACK. THE SIGNAL CABLE LENGTH FROM THE FFD MODULES TO THE READOUT ELECTRONICS IS 8 M.

IN SUMMARY, THE READOUT ELECTRONICS SYSTEM PLAYS A CRUCIAL ROLE IN THE PRECISE DATA COLLECTION AND EFFICIENT CONTROL OF FFD AND TOF DETECTORS, ENSURING THE RELIABILITY AND ACCURACY OF RESULTS OBTAINED IN PARTICLE PHYSICS EXPERIMENTS.

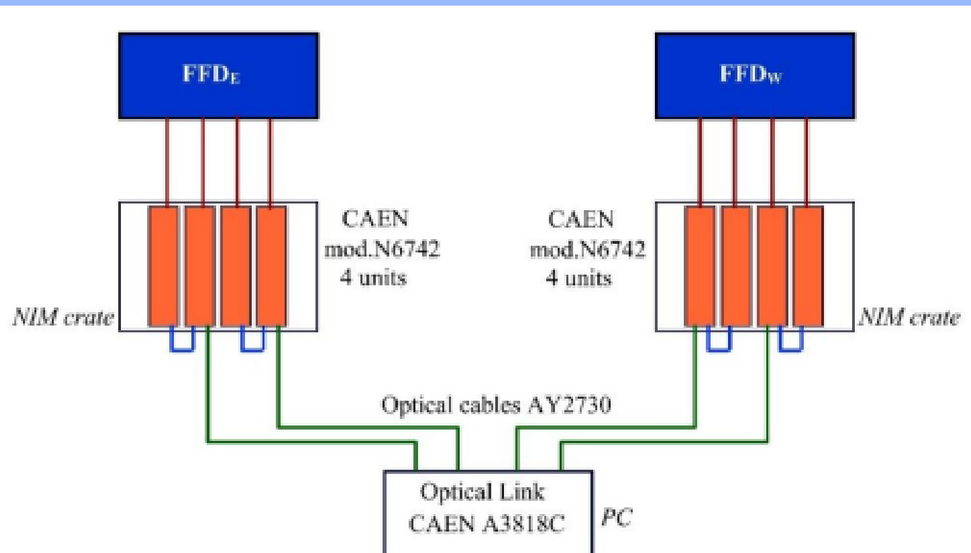

REFERENCES
[1] R. A. KADO ET AL., “THE CONCEPTUAL DESIGN OF THE MINIBEBE DETECTOR PROPOSED FOR NICA-MPD,” JINST,
VOL. 16, NO. 02, P. P02002, 2021.
[2] M. COLLABORATION, “MPD-ITS TECHNICAL DESIGN REPORT -V1.01,” 2022.
[3] “EXPERIMENTAL METHODS AND COLLIDERS,” PHYSICS LETTERS B, VOL. 592, NO. 1, PP. 235–274, 2004. REVIEW OF
PARTICLE PHYSICS.

REFERENCES
[1] R. A. KADO ET AL., “THE CONCEPTUAL DESIGN OF THE MINIBEBE DETECTOR PROPOSED FOR NICA-MPD,” JINST,
VOL. 16, NO. 02, P. P02002, 2021.
[2] M. COLLABORATION, “MPD-ITS TECHNICAL DESIGN REPORT -V1.01,” 2022.

"WITH SPECIAL GRATITUDE AND HONOR TO:
M. ALVARADO, A. AYALA, M. HERRERA, I. MALDONADO, E. PATI˜NO, A. RAYA,